REVIEW

Recent Research Progresses of Solid-State Lithium-Sulfur Batteries

Yu Luo [a,#], Ru-Qin Ma [a,#], Zheng-Liang Gong [b,*], Yong Yang [a,b,*]

[a] State Key Laboratory for Physical Chemistry of Solid Surface, College of Chemistry and Chemical Engineering, Xiamen University, Xiamen, 361005, Fujian, China
[b] College of Energy, Xiamen University, Xiamen, 361005, Fujian, China

Abstract

All solid-state lithium-sulfur batteries (ASSLSBs) are considered to be one of the most promising next-generation energy storage systems, due to the promises of high energy density and safety. Although the use of solid-state electrolytes could effectively suppress the "shuttle effect" and self-discharge of the conventional liquid lithium-sulfur (Li-S) battery, the commercialization of ASSLSBs has been seriously hampered by the electrolyte degradation, electrode/electrolyte interfacial deterioration, electrochemo-mechanical failure, lithium dendrite growth and electrode pulverization, etc. This paper provides a comprehensive review of recent research progresses on the solid-state electrolytes, sulfur-containing composite cathodes, lithium metal and lithium alloy anodes, and electrode/electrolyte interfaces in ASSLSBs. Specifically, lithium sulfide and metal sulfide as new active cathode materials, and lithium alloy as new anode materials are overviewed and analyzed. In addition, some newly developed interfacial modification strategies for addressing the electrode/electrolyte interfacial challenges are also outlined. Furthermore, an outlook on the future research and development of high-performance ASSLSBs are also presented.

Keywords: Lithium-sulfur batteries; Solid-state electrolytes; Interfacial compatibility; Triple-phase interfaces; Electrochemo-mechanical effects

1. Introduction

To address the urgent challenge of global warming, the realization of carbon neutrality and the construction of a sustainable society are the common goals of human society. Under this premise, secondary batteries with high specific energy are one of the favorable means to support the technology development for reduce carbon emissions and alleviate environmental pressure. With the continuous developments in the lithium-ion batteries (LIBs) technologies, the energy density of conventional LIBs has significantly increased and gradually approached the theoretical limit. Therefore, the development of new and innovative systems beyond LIBs, such as lithium-sulfur (Li-S) batteries and lithium-air batteries, is highly desirable for green transportation, renewable electricity and the grid applications.

Sulfur, which is abundant, low-cost, environmentally friendly and nontoxic, has a high theoretical specific capacity of 1672 $mAh \cdot g^{-1}$. When coupling with Li metal anode (3800 $mAh \cdot g^{-1}$), Li-S batteries (LSBs) have a high specific energy of up to 2600 $Wh \cdot kg^{-1}$. However, the commercialization of LSBs still faces many challenges, including the shuttle effect, the volume change during cycling, the insulating properties of S/Li_2S, resulting in low utilization of active materials and large voltage polarization, poor stability of electrode structure and other problems, which make the assembled LSBs face the dilemma of poor cycle performance, low coulombic efficiency, serious self-discharge. When using lithium metal anode, there are also many challenges, including lithium dendrite growth, "dead lithium" generation and electrode pulverization induced by volume change during

Received 23 August 2022; Received in revised form 14 September 2022; Accepted 6 October 2022
Available online 8 October 2022

* Corresponding author, Zheng-Liang Gong, Tel.: (86-592) 2880703, E-mail address: zlgong@xmu.edu.cn.
* Corresponding author, Yong Yang, Tel.: (86-592) 2185753, E-mail address: yyang@xmu.edu.cn.
[#]Yu Luo and Ru-Qin Ma contributed equally to this work.

https://doi.org/0.13208/j.electrochem.2217007

cycling, which will cause such problems as short circuit and voltage polarization increased. As a result, the energy density and the cycle life of LSBs are reduced, and its advantages cannot be exerted. In order to overcome the above problems, researches have been carried out in the modification of LSBs through the use of electrolyte additives, binder optimization, separator modification, interface modification, structure design. However, the above methods can often only solve some of the problems. Replacing liquid electrolytes (LEs) with solid-state electrolytes (SSEs) getting theoretically high ionic conductivity, wide electrochemical window, and sufficient mechanical strength to construct all solid-state Li-S batteries (ASSLSBs) is an ideal strategy to achieve both high energy density and high safety [1,2].

Nowadays, different kinds of SSEs have been applied in ASSLSBs, such as polymer-based electrolytes, oxide-based electrolytes, sulfide-based electrolytes, and inorganic-organic composite electrolytes, which will be elaborated in Section 2. ASSLSBs using different SSEs will undergo different electrochemical reaction processes. For example, in the polymer-based ASSLSBs, the conversion of S to Li_2S will undergo a "solid-liquid-solid" multi-step reaction process similar to that in liquid lithium-sulfur batteries, which leads to the shuttle effect still a major problem. When using inorganic electrolytes such as oxide or sulfide-based electrolytes, S and Li_2S undergo a direct "solid-solid" single-step reaction process, as shown in Fig. 1. The solid-solid conversion between S and Li_2S effectively avoids the formation of lithium polysulfides (LiPSs) intermediates and thus, prevent various problems caused by the shuttle effect, but it also leads to the problems of sluggish kinetics and low utilization of active materials. Therefore, the cathode structure needs to be rational designed. The inorganic SSEs-based ASSLSBs have no liquid components, thus avoiding the risk of electrolyte leakage, and effectively improving the battery safety. However, inorganic electrolytes also have problems, such as low ionic conductivity, narrow electrochemical stability window and poor chemical stability, that need to be solved [3,4].

The challenges in volume change and structural stability of the composite cathode also need big attention in ASSLSBs systems (Fig. 1(B)), which includes "chemo-mechanical failure", "electrolyte degradation" and "tortuous carriers transport" [5]. Large volume changes lead to the "contact-loss" of the components in the composite cathode, even inducing cracks and pulverization by the local stress. As a result, as the cycle progresses, the triple-phase interface becomes less and less, resulting in the loss of electrical contact between the active material and the conductive channel [1]. Thus the "chemo-mechanical failure" makes the capacity gradually decays. Mechanical ball milling, especially high-energy ball milling, can reduce the particle size of isolated sulfur compared with manual milling, thereby reducing the impact of volume changes, dispersing the components more uniformly and constructing more triple-phase interfaces [6]. Although the degradation of the electrolyte in the working voltages range of 1.5-3.0 V will not be as severe as that of the high voltage cathode system like high-nickel layered oxide cathode, the degradation of the electrolyte will still occur due to the limited electrochemical stability window of sulfide SSEs, resulting in the formation of an interfacial layer. The inert interfacial layer will block the transport of ions, resulting in increased polarization and degradation of battery capacity [5]. Last but not least, the tortuosity of cathode in ASSLSBs is very important, which determines the overall rate capability. Depending on the microstructure of the individual components of the composite electrode, especially in thick electrodes, sluggish ion/electron transport increases overpotential [7]. In fact, these failure mechanisms are often coupled with each other, for example, sluggish ion transport can be further worsened by electrolyte degradation, formation of inert interphases, or cracks.

This review systematically summarizes recent researches on SSEs, sulfur and sulfide-containing composite cathodes, lithium metal/alloy anodes, and electrode/electrolyte interfaces, and provides an outlook for future research on ASSLSBs.

2. Solid-state electrolytes

SSEs are important components for the development of high-safety, high-energy-density solid-state lithium-sulfur batteries, and act as both a separator and a Li^+ conductor. So far, researchers have developed polymer-based electrolytes, oxide-based electrolytes, sulfide-based electrolytes and composite SSEs.

2.1. Polymer-based SSEs

Polymer-based electrolytes have the advantages of suitable electrochemical window and flexibility. However, they also suffer from poor room temperature ionic conductivity (typically 10^{-8}–10^{-6} $S \cdot cm^{-1}$), low mechanical strength, and shuttle effect. Polymer-based electrolytes can be divided into gel polymer electrolytes (GPEs) and solid polymer electrolytes (SPEs) depending on

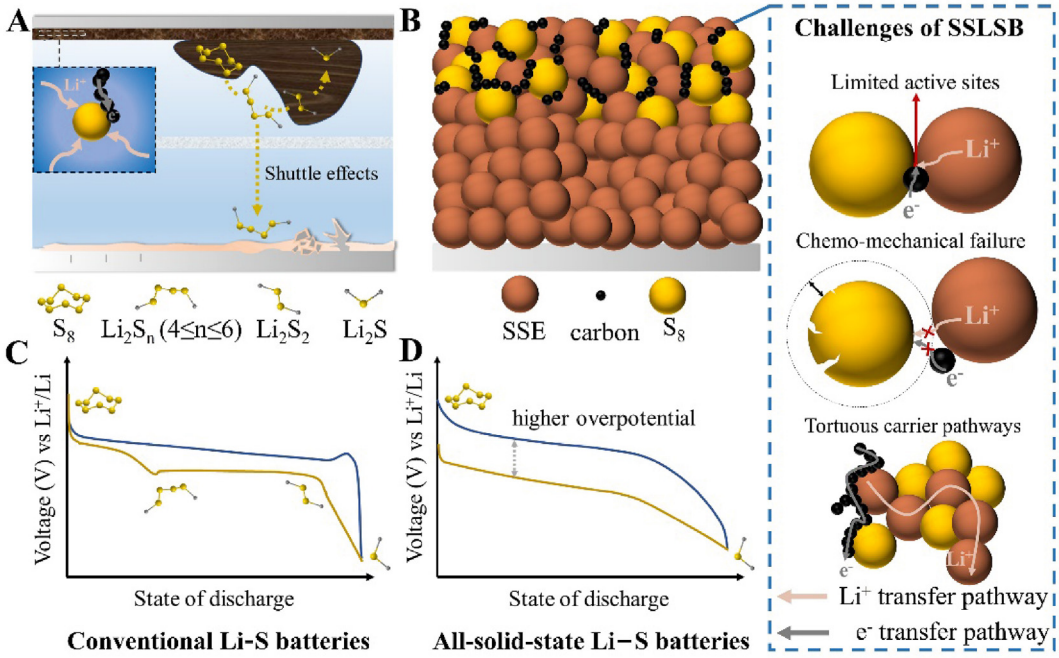

Fig. 1. Schematic illustrations of (A) conventional Li-S batteries and (B) all-solid-state Li-S batteries and significant challenges to be solved (in the dashed box). Charge and discharge curves of (C) conventional Li-S batteries and (D) all-solid-state Li-S batteries.

whether electrolytes or solvents are added. Due to the liquid components, GPEs have the advantages of flexibility and high ionic conductivity comparable to liquid electrolytes, but there are safety issues when paired with Li metal anodes. In view of this, SPEs which contain no liquid components have received extensive attention, but their low room-temperature ionic conductivity limits their application. In most cases, SPEs-based ASSLSBs need to be operated at high operating temperatures above 60 °C. At the same time, due to poor mechanical properties, SPEs are difficult to inhibit Li dendrite growth at the normal operating temperature of batteries, thus the battery failure problem will occur. Besides, the shuttle effect still exists in polymer-based batteries due to the high solubility of LiPSs in common polymer matrices.

2.1.1. Improve ionic conductivity

The rapid migration of lithium ions in polymer-based electrolytes relies on the "complex-decomplex-recomplex" between lithium ions and oxygen atoms on the polyethylene oxide (PEO) segment in the amorphous region. However, polymer-based electrolytes are easy to be crystallized, thus many studies have focused on the modification of the structure of polymer-based electrolytes, such as lithium salts [8], cross-linking [9,10], inorganic fillers [11,12], organic-inorganic hybrids [13,14] and so on, to improve ionic conductivity.

Adding organic/inorganic nanofillers to the polymer matrix can reduce its crystallinity and improve its ion transport and mechanical properties. Wang et al. [12] pointed out that the organic nanofiller-polymer composite electrolytes have higher mechanical/thermal stability and lower LiPSs solubility. Wang et al. [15] used a low-molecular-weight polymer, hydrolyzed polymaleic anhydride (HPMA), as an organic solid filler to greatly enhance the ionic conductivity of PEO-based SPEs through suppressing PEO crystallinity. The prepared PEO-1%HPMA SPE shows an ionic conductivity of 1.13×10^{-4} S·cm^{-1} at 35 °C. At the same time, PEO-1%HPMA SPE exhibits better mechanical properties, higher thermal stability, wider electrochemical working window and higher stability to lithium metal, which effectively improves the performance of the SPE.

In addition to organic fillers, some commonly used inorganic fillers can also be used, which are mainly divided into inert fillers that do not conduct Li^+ intrinsically and active fillers that conduct Li^+. This section mainly introduces the former one, and the content of active fillers will be introduced in Section 2.2. Sheng et al. [16] described that the physically mixed inorganic nanoparticles are isolated in the polymer matrix, and ion transport is still restricted by Li^+ jumping along the PEO chains. To address this problem, an ion-conducting interface can be designed to further enhance Li^+ transport. They enhanced Li^+ transport by designing an

effective interface of nanofiller/polymer/lithium salt. Cai et al. [17] demonstrated that ionic conductivity can be effectively improved by enhancing the interaction between nanofillers and polymers to change the local environment of Li^+, thereby facilitating the movement of Li^+. By introducing acrylamide (AM) into the PEO-based solid electrolyte, the abundant polar groups bring multiple hydrogen bonding forces to the system, the lithium interaction force has been changed from the original single Li···O−C to the coexistence of multiple lithium effects (Li···O−C, Li···O=C, and Li···N−H). The widening of the ion transport channel and the shortening of the migration path effectively increase the ion conductivity of the electrolyte. SiO_2 is modified to obtain the double bond modification of nanosilica (=SiO_2) as a nano-crosslinking agent. When AM and poly (ethylene glycol) methyl ether methacrylate (PEGMA) are polymerized on the surface of SiO_2 nanoparticles, they can be used as Li^+ transport carriers, so that Li^+ can be transported not only between adjacent SiO_2 nanoparticles, but also on the surface of =SiO_2. Both methods enriched the Li^+ transport path, greatly shortened the Li^+ transport distance, thus effectively improved the ionic conductivity. The room temperature ionic conductivity of the modified SPE is 2.6×10^{-4} S·cm^{-1}, which is improved by about 3 orders of magnitude, and the Li^+ transfer number reaches 0.84, which is much higher than the unmodified 0.26 (Fig. 2(A)).

In addition, ionic conductivity can also be improved by designing some new types of salts. Zhang et al. [18] constructed a stable LiF-rich solid electrolyte interface (SEI) on the Li metal anode side by replacing one F atom in $-CF_3$ with H atom in the commonly used salt (difluoromethanesulfonyl) (trifluoromethanesulfonyl)imide anion (DFTFSI), and at the same time, the ionic conductivity of the electrolyte was also improved. Wang et al. [19] prepared cyclopropenium cationic-based covalent organic polymer (iCP@TFSI) through the SN_2 reaction and ion replacement process (iCP@Cl to iCP@TFSI). Their SPE was prepared with iCP@TFSI as a filler. The prepared SPE has good mechanical properties and high stability to Li metal anode. And at the same time, due to the existence of cationic framework, the Li^+ migration number and Li^+ conductivity are increased. The as-prepared PEO-10%iCP@TFSI exhibits an ionic conductivity of 1.3×10^{-3} S·cm^{-1} at 80 °C (Fig. 2(B)).

2.1.2. Suppress the shuttle effects and self-discharge

It is worth noting that due to the high solubility of LiPSs in polymers, polymer-based electrolytes [20] and even polymer-based composite electrolytes [21,22] cannot completely inhibit LiPSs shuttling. Due to the shuttle effect, the polymer-based ASSLSBs suffer from self-discharge problem. Designing polar functional groups to adsorb and immobilize LiPSs [23], electrolyte interlayers that can inhibit the shuttling of LiPSs [24], and applying redox mediators/catalysts to accelerate the conversion reaction kinetics of LiPSs [25] have been extensively explored to address this challenge.

Through X-ray photoelectron spectroscopy, *in-situ* optical microscopy, and three-electrode measurement, Liu et al. [24] found that in polymer-based solid electrolytes, sulfur will also be dissolved and diffused, and unevenly distributed on the surface of the anode, leading to the inhomogeneous Li^+ plating/stripping at the anode/SPE solid-solid interface, resulting in obvious overpotential fluctuations. In view of this, they prepared an interfacial layer composed of super-aligned carbon nanotube (SACNT) films, GO, and SPE to prevent Li metal from reacting with LiPSs to prolong battery life (Fig. 3(A)).

Liu et al. [26] synthesized polymer with intrinsic microporosity and applied as an organic framework to comprehensively enhance the performance of PEO by forming a composite electrolyte (PEO-PIM). The electrophilic 1,4-dicyanooxanthrene functional groups contained in PIM possess higher binding energy to LiPSs, thus it can effectively adsorb LiPSs and inhibit the shuttle effect. Assembled Li-S battery has an initial specific capacity of 1181 mAh·g^{-1} with a capacity retention rate of 61.8%.

Besides reducing the shuttle effect of LiPSs by confinement, it can also be controlled by accelerating the conversion between sulfur species on the cathode side. Therefore, many strategies such as catalysis and addition of redox mediators (RM) developed in liquid lithium-sulfur batteries can also be directly applied to polymer systems. Gao et al. [25] enhanced the reaction kinetics of sulfur species by adding redox mediator of soluble-type quinone-based RM (1,5-bis(2-(2-(2-methoxyethoxy)ethoxy) ethoxy) anthra-9,10-quinone, AQT) to accelerate interfacial charge transfer (Fig. 3(B)).

2.2. Oxide-based hybrid SSEs

Oxide SSEs, which comprises the NASICON type, garnet type and perovskite type electrolytes, exhibit wide voltage window and high ionic conductivity (10^{-4}—10^{-3} S·cm^{-1} at room temperature) [27]. However, due to its high rigidity, it cannot form a good mechanical contact with the conversion-type cathodes which endure a large volume change. During cycling, the loss of contact between

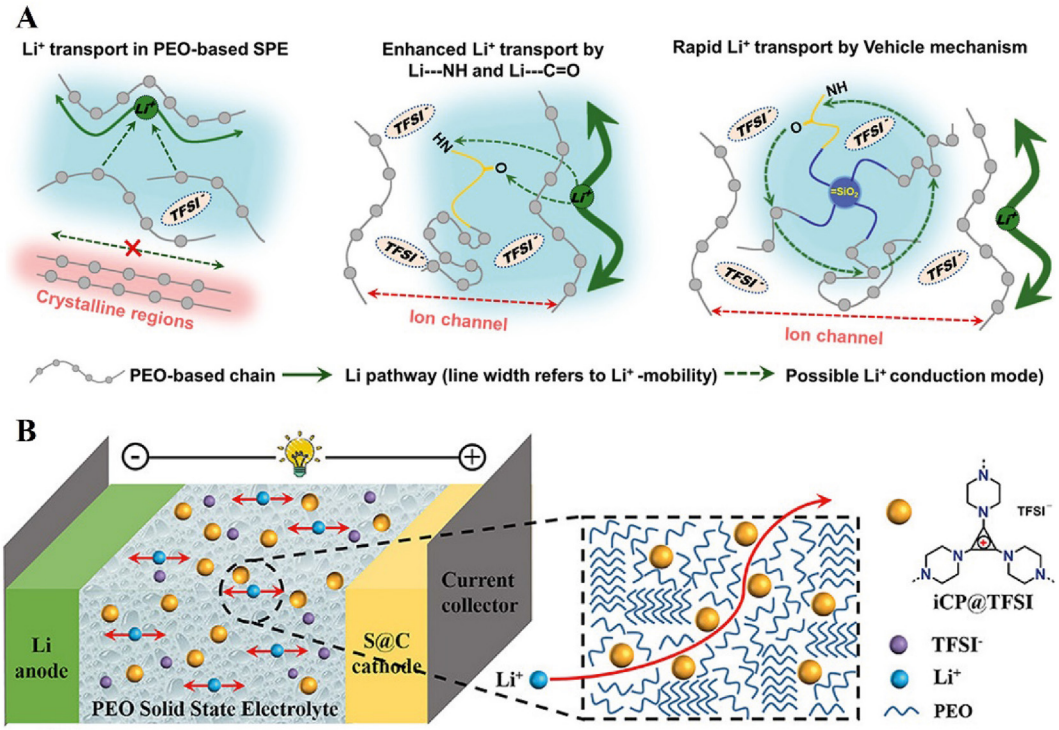

Fig. 2. Schematic illustrations of lithium-ion conduction mechanism diagram in (A) P-P, P-P-A, P-P-A@SiO_2 SPEs [17] and (B) iCP@TFSI SPE [19]. Copyright with 2021 American Chemical Society and Copyright with 2021 American Chemical Society.

the active material and the ion-conducting channel will result in increasing of interfacial impedance. In practice, oxides are usually combined with LEs, ionic liquid or polymer electrolytes to obtain composite electrolytes to enhance the interfacial contact, in which the characteristics of oxide electrolyte (safety and high mechanical strength) are well preserved.

2.2.1. Composite strategies

Appropriate composite strategies have significant effects on the electrochemical performance of composite electrolytes. For instance, direct composite strategy is the simplest way. AbdelHamid et al. [28] processed 3D sheet $Li_7La_3Zr_2O_{12}$ (LLZO) with polytetrafluoroethylene (PTFE) to obtain a non-rigid solid framework, then prepared hybrid quasi-solid electrolyte (HQSE) by injecting LE with LiTFSI in a mixture of dimethoxyethane (DME) and 1,3-dioxolane (DOL). LLZO electrolyte can effectively adsorb anions and inhibit their movement, thus exhibiting a higher Li^+ transference number than LEs. Besides, the leakage of injected LE is prevented due to the porous property of the solid framework, so the thermal stability of the HQSE is also much higher than that of the ordinary Cergard separator. Nevertheless, the direct composite strategy is hard to realize the uniform compositing of oxide ceramic and polymer, in which the interfacial resistance between ceramic and polymer phases severely restricts the ionic conductivity.

In view of this, *in-situ* polymerization can be applied to composite the polymer directly on the ceramic to form closer contact. The crystallinity of the polymer can also be reduced due to the addition of inorganic fillers, which effectively improves the ionic conductivity of the polymer electrolyte, thereby improving the utilization of active materials. Yu et al. [29] prepared composite polymer electrolyte (CPE) containing polyethylene glycol diacrylate (PEFDA), LE and $Li_{6.4}La_3Zr_{1.4}Ta_{0.6}O_{12}$ (LLZTO) by *in-situ* thermal polymerization. Although there is still a small amount of LE in the system, the presence of LLZTO effectively improves the flame retardancy and thermal stability of CPE, thus ensuring high safety. At the same time, CPE can also inhibit the shuttle effect and the growth of Li dendrites. The assembled Li-S battery delivers an initial discharge capacity of 1201 $mAh \cdot g^{-1}$ at 1C, retaining 656 $mAh \cdot g^{-1}$ after 200 cycles.

After composing, it is also necessary to pay attention on the overall stability of the electrolyte. Bag et al. [30] improved the stability of polyvinylidene fluoride (PVDF) to Li metal by adding LiF to the PVDF-garnet type LLZTO composite electrolyte.

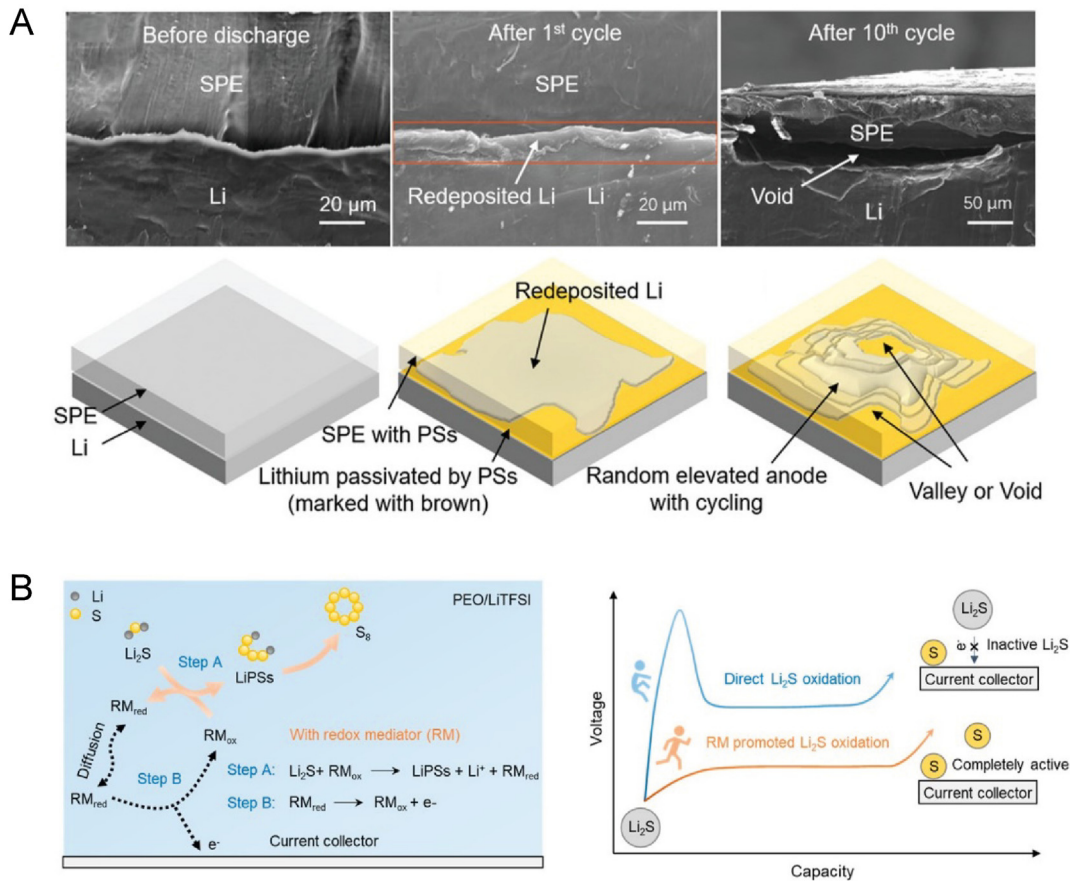

Fig. 3. (A) Cross-section SEM images of the Li anode-SPE interface in the S/SPE/Li cell and schematic illustration of Li redeposition process and the cell failure mechanism [24]; (B) The schematic illustrations of RMs for ASSLSBs [25]. Copyright with 2021 Wiley-VCH GmbH and Copyright with 2021 American Chemical Society.

2.2.2. Inorganic skeleton morphology

The morphology of oxides in composite electrolytes has important effects on the electrochemical performance of the CPEs. Nanoparticles have larger specific surface areas, which can achieve better interfacial properties. Functionalizing the surface of nanoparticles is a promising approach to overcome the challenge of high resistance at the composite interface. Li et al. [31] grafted the molecular brush (MB) on the surface of LLZTO nanoparticles and then composited it with PEO. They observed the Li^+ transportation between the interface by ^6Li direct polarization nuclear magnetic resonance (NMR) spectra, demonstrating an interface-assisted ion transport mechanism. ASSLSBs based on MB-LLZTO-CPE electrolyte exhibits a discharge capacity of 1280 $mAh \cdot g^{-1}$ and relatively stable cycling performance. In addition, the macrostructure design of nanoparticles can also be performed to develop multilayer SSEs with different functions. Yan et al. [32] embedded LLAZO nanoparticles into carbon nanofibers (CNFs) to prepare a functional electrolyte-cathode framework structure containing continuous LLAZO channels, which effectively shortens the transport pathways of charge carrier.

Apart from nanoparticles, continuous inorganic substrates can also be constructed to form channels for fast transport of Li^+. Kou et al. [33] prepared a PEO-impregnated $Li_{0.33}La_{0.557}TiO_3$ (LLTO) electrolyte with porous and dense layers. The continuous LLTO framework effectively enhances the ionic conductivity. The existence of the dense layer can effectively improve the compressive strength, and make Li^+ deposit uniformly, while the PEO in the porous layer enhances the flexibility and processability of the electrolyte. The assembled Li-S battery delivers an initial discharge capacity of 1234.6 $mAh \cdot g^{-1}$ at 60 °C, and after 100 cycles, there is still 907.6 $mAh \cdot g^{-1}$ with a CE of nearly 99%.

2.3. Sulfide SSEs

Among the currently developed SSEs, sulfide solid-state electrolyte (namely sulfides) has the highest ionic conductivity (10^{-3}–10^{-2} $S \cdot cm^{-1}$) and low activation energy (0.15–0.35 eV), due to the

stronger polarizability of S^{2-} and good mechanical properties [28]. Compared with oxides, their grain boundary and interfacial impedance are much lower. Sulfide solid electrolytes can be classified as glassy, glass-ceramics (formed by partial crystallization of glassy electrolytes), and ceramic solid electrolytes [2]. (1) Glassy sulfide electrolyte: the widely investigated glass sulfides are the binary $xLi_2S\cdot(100-x)P_2S_5$ system (x = mole percentage). The typical binary glassy sulfide SSEs have isotropic structure and readily ion conduction. The physicochemical properties of the binary glassy sulfide electrolyte system can be tuned by adjusting the ratio of its composition [34]. (2) Glass-ceramics sulfide electrolyte: the so-called "glass-ceramics" sulfide SSEs are partially crystallized from glassy sulfide through the heat treatment of the glassy SSEs at a relatively low temperature (below 300 °C), thus exhibiting a higher ionic conductivity of ca. 10^{-3} $S\cdot cm^{-1}$. Mizuno et al. [35] found that the crystallized Li_2S-P_2S_5 glass-ceramic exhibits an ultra-high ionic conductivity of 3.2×10^{-3} $S\cdot cm^{-1}$ at room temperature. Due to the formation of the highly-conductive metastable crystalline $Li_7P_3S_{11}$ phase, the ionic conductivity is improved, which indicates that the formation of the highly-conductive phase plays a key role in improving the ionic conductivity of the Li_2S-P_2S_5 glass-ceramic electrolyte. Another method to improve the ionic conductivity of Li_2S-P_2S_5 glass-ceramic electrolytes is to further eliminate voids and grain-boundaries in the SSEs by hot pressing, thereby reducing the grain boundary resistance. The Li_2S-P_2S_5 glass-ceramic electrolyte prepared by hot pressing [36] shows a high ionic conductivity of 17 $mS\cdot cm^{-1}$ with a low activation energy of 17 $kJ\cdot mol^{-1}$ (3) Ceramics sulfide electrolyte: ceramics sulfides can be divided into argyrodite Li_6PS_5X (X = Cl, Br, I) and thio-lithium superionic conductor (LISICON) family, expressed by the general formula $Li_xM_{1-y}M'_yS_4$ (M = Si, Ge, Sn, Zr; M' = P, Al, Zn, Ga, Sb; $0<x<1$). The thio-LISICON family possess higher ionic conductivity due to the larger radius and stronger polarization of sulfide ions [37,38]. As for Li_6PS_5X, Viallet et al. [39] reported the room-temperature ionic conductivities of Li_6PS_5Cl, Li_6PS_5Br, and Li_6PS_5I are 4.6×10^{-4} $S\cdot cm^{-1}$, 6.2×10^{-4} $S\cdot cm^{-1}$, and 1.9×10^{-4} $S\cdot cm^{-1}$, respectively. Li_6PS_5I consists of fully ordered S^{2-} and I^-, Li_6PS_5Cl consists of fully disordered S^{2-} and I^-, and Li_6PS_5Br is a mixture of ordered and disordered structures, thus Li_6PS_5Br exhibits the fastest Li^+ conduction. In order to further improve ionic conductivity and air-and-moisture stability, a batch of pseudo-quaternary SSEs have been developed in recent years, e.g., Li_2S+P_2S_5+MS_2+LiX (M = Ge, Sn, Si, Al, etc.; X = F, Cl, Br, I). In 2016, Kanno et al. [40] reported a novel fast lithium superionic conductor $Li_{9.54}Si_{1.74}P_{1.44}S_{11.7}Cl_{0.3}$, which possesses a 3D conductive network and thus exhibits an ionic conductivity of 25 $mS\cdot cm^{-1}$. Liang et al. [41] prepared a series of Sb-doped LGPS electrolytes ($Li_{10}Ge(P_{1-x}Sb_x)_2S_1$), which not only possessed a high ionic conductivity (18 $mS\cdot cm^{-1}$), but also improved air stability because the soft acid Sb partially replaces P, which can form a stronger covalent bond with S. By tuning the structure with doping, substitution, or changing the stoichiometric ratio, the ionic conductivity of SSEs is significantly improved to 10^{-2} $S\cdot cm^{-1}$, which is able to meet the requirements for practical use in solid-state batteries. With these advantages, sulfides can be applied as stand-alone electrolyte in ASSLSBs. However, on the cathode side, due to the insulating nature of sulfur, composite cathode is often made by mixing sulfides, carbon and sulfur to provide ionic and electronic conduction channels. Therefore, it is still meaningful to further improve the ionic conductivity of sulfide electrolytes [42−47]. Wei et al. synthesized $Li_{5.5}PS_{4.5}Cl_{1.5}$ by enriching Cl on the basis of Li_6PS_5Cl through a simple solid-phase ball milling method, achieving a high level ionic conductivity of 8.7 $mS\cdot cm^{-1}$ (Fig. 4(A)) [47].

2.3.1. Electrochemical stability

A major problem currently faced by sulfides is the narrow electrochemical window, which leads to the degradation and hindering ion transport at the interface. It is more accurate to use Li/SSE/SSE-carbon to evaluate the inherent electrochemical window of SSE, which is consistent with the theoretical calculation result [48,49]. Limited by the oxidation of S^{2-} and the reduction of high valence cations (P^{5+}, Ge^{4+}, etc.), the electrochemical window of sulfide SSEs is generally narrow. At present, there are two main ways to widen the sulfide voltage window, O doping and the construction of passivation layer [50]. O doping can improve the structural stability, but at the same time, it inevitably reduces the ionic conductivity [51]. It is feasible to construct a thin coating layer to inhibit the degradation of the sulfide SSE [52]. The appropriate coating method is very important, which can resist the interfacial reaction without hindering the smooth transport of ions.

2.3.2. Chemical stability

The poor air stability and compatibility in slurry-based processes is the major bottleneck limiting large-scale application of sulfides. Water will react

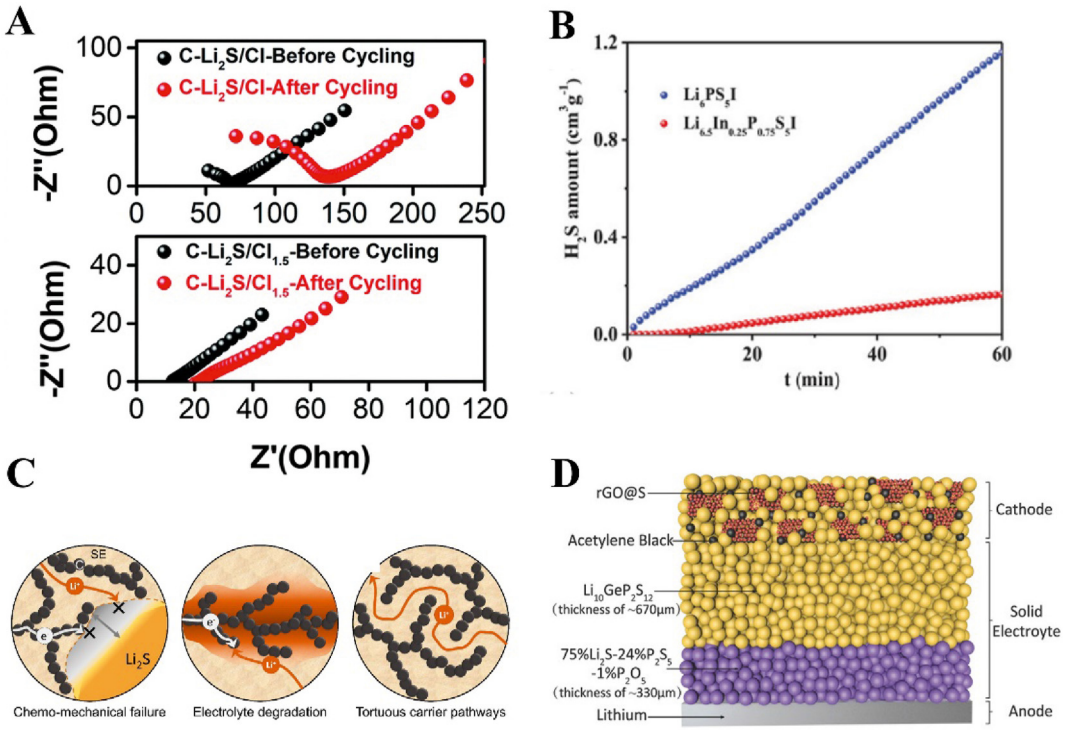

Fig. 4. (A) EIS plots of C-Li_2S/Li_6PS_5Cl/In-Li and C-Li_2S/$Li_{5.5}PS_{4.5}Cl_{1.5}$/In-Li solid-state batteries before and after 65 cycles at room temperature [47]. (B) The quantity of H_2S gas produced from $Li_{6.5}In_{0.25}P_{0.75}S_5I$ and Li_6PS_5I when exposed in moisture air [54]. (C) Significant challenges to solve for solid-state Li-S batteries [6]. (D) Schematic diagram of an all-solid-state Li-S battery composed of rGO@S-AB-LGPS composite cathode [56]. Copyright 2021 Wiley-VCH GmbH, Copyright with 2021 American Chemical Society and Copyright with 2017 WILEY-VCH Verlag GmbH & Co. KGaA, Weinheim.

with the sulfide electrolyte to form H_2S, which will lead to degradation of the sulfides. Strategies for improvement include using additives, employing the hard and soft acids and bases (HSAB) principle to dope, designing core-shell structure [53]. Based on the HSAB principle and DFT calculation guidance, Zhao et al. [54] doped In in Li_6PS_5I electrolyte to improve air stability. In their work, $Li_{6.5}In_{0.25}P_{0.75}S_5I$ was rapidly synthesized in one pot by the ultimate-energy mechanical alloying (UEMA) method. The air exposure experiment shows that the amount of H_2S released by the $Li_{6.5}In_{0.25}P_{0.75}S_5I$ electrolyte decreases sharply (Fig. 4(B)). Tufail et al. [55] prepared $Li_{6.95}Zr_{0.05}P_{2.9}S_{10.8}O_{0.1}I_{0.4}$ electrolyte by co-doping ZrO_2 and LiI. O doping contributes to the formation of POS_3^{3-} and $P_2OS_6^{4-}$ structural units, which effectively improves the air stability.

2.4. Other SSEs

To overcome the problems faced by oxide-based electrolytes (low ionic conductivity, rigidity) and sulfide-based electrolytes (narrow electrochemical window and poor air stability), halide-based electrolytes with wider voltage window, higher ionic conductivity and ductility have received extensive attention.

The essence of halide-based electrolytes is to replace Li in LiX (X = F, Cl, Br, I) with multivalent cations or replace X with multivalent anions to obtain intrinsic vacancies, thereby achieve higher ionic conductivity [57]. For anti-perovskite halide electrolytes obtained by substitution X with multivalent inorganic anions, they usually have a relatively narrow electrochemical window [58]. For metal halides, as the period of halogen elements increases, the ionic conductivity also increases gradually due to the difference between its ionic radius and lithium ion, but the oxidation resistance gradually decreases. Among them, although the fluoride-based electrolyte $LiMF_4$ has a high oxidation potential (over 6 V vs. Li/Li^+), the reported ionic conductivity has not yet exceeded 1×10^{-3} $S \cdot cm^{-1}$. Bromide-based and iodide-based electrolytes have high ionic conductivity, but poor structural stability, and the upper voltage limit is only 3 V (vs. Li/Li^+), which is the same dilemma as sulfide-based electrolytes, and it is difficult to achieve high ionic conductivity and wide voltage window at the same time. In contrast, the chloride-based electrolytes Li_3MCl_6 or $Li_2M_{2/3}Cl_4$ can achieve a good balance between ionic conductivity and electrochemical stability, and can achieve 10^{-3} $S \cdot cm^{-1}$ level ionic conductivity at room

temperature. The voltage window above 4 V (vs. Li/Li^+) reflects the advantages over sulfide-based electrolytes, thereby Li-M-Cl-type halide-based electrolytes have attracted extensive attention.

Shi et al. [59] synthesized the halogenated-based electrolyte Li_3HoBr_6 (LHB) by solid-phase method, and the obtained LHB electrolyte exhibits an electrochemical window of 1.5−3.3 V (vs. Li/Li^+) and high ionic conductivity (1.1×10^{-3} $S \cdot cm^{-1}$) at room temperature, and can be well cold pressed into sheets.

3. Cathodes materials

Unlike liquid Li-S batteries, all solid-state Li-S batteries undergo direct electrochemical conversion between sulfur and lithium sulfide, without the generation of lithium polysulfide intermediates, so the shuttle effect can be fundamentally eliminated, thus effectively improving the cycle life and suppressing self-discharge. However, this also leads to the problems of sluggish kinetics and low active material utilization of the batteries. Meanwhile, as mentioned above, LiPSs has a high solubility in polymer-based electrolytes, so the shuttle effect still needs to be suppressed in polymer-based all solid-state Li-S batteries. The commonly used cathode active materials include elemental sulfur, lithium sulfide and various metal sulfides.

3.1. Sulfur as active materials

Due to its high specific capacity, high natural abundance, low cost, and environmental friendliness, sulfur is the most widely used cathode active materials. However, sulfur as the active materials also faces many challenges. One of the challenges is that both S and its discharge product Li_2S have low electronic and ionic conductivities, the electrochemical reaction of active materials relies on the ion and electron transports through the triple-phase interfaces among active materials, SSEs and conductive additives [60]. Owing to lack of the infiltration and wetting of liquid-electrolyte, Li^+ transport at the electrode/electrolyte interface is considered as a limiting factor for the electrochemical conversion process of the active species, while the need of a sufficiently number of triple-phase interfaces also poses new requirements for the design of carbon materials. Another problem faced by sulfur cathodes is the huge volume expansion (ca. 80%) during charge-discharge cycling due to the density difference between S and Li_2S, which will lead to chemical-mechanical failure problems. At the same time, since the construction of the triple-phase interface of the composite cathode is usually through simple mechanical mixing, it will lead to tortuous ion transport pathways in the composite cathode, resulting in poor Li^+ transport properties [6] (Fig. 4(C)).

3.1.1. Strategies of improving kinetics

Due to the electrically/ionically insulating nature of S and Li_2S and the poor solid-solid contact in the composite cathode, ASSLSBs suffer from slow reaction kinetics and low active material utilization. Many studies have been conducted to enhance the performance of ASSLSBs by constructing ion/electron conducting channels [56] to enhance the active material conductivity.

By combining S with carbon materials, on the one hand, the electronic conductivity of the composite cathode can be effectively improved, and on the other hand, the volume change of S can be alleviated. By depositing S on the surface of CNTs, Zhang et al. [61] effectively alleviated the volume expansion of S during cycling, reduced the interfacial stress/strain, and improved the interfacial stability, thereby improving the cycling stability of the battery.

Yao et al. [56] deposited nano-amorphous sulfur on rGO through a sulfur-amine chemistry method, which effectively promoted the electron conduction at the interface. The uniform distribution of the rGO@S nanocomposite promoted subsequent electron/ion transport, generating uniform volume changes during lithiation/delithiation (Fig. 4(D)).

Although the introduction of conductive carbon can effectively improve the battery performance, the routine point-to-point contact between sulfur and conductive carbon in the above work still limits the performance improvement. In view of this, Hou et al. [62] effectively changed the routine point-to-point contact into a unique surface-to-surface interfaces between active sulfur and conductive CNTs skeleton by adding a heat treatment after the ball milling of S and CNTs, which resulted in a closer contact between the active material and the conductive network. This improves the electron transfer at the solid-solid interface, effectively reduces the formation of "dead sulfur" and mitigates the volume change during cycling. The interfacial impedance is reduced and the reaction kinetics is effectively improved, thus the utilization of the active material is enhanced. An initial discharge capacity of 1138.7 $mAh \cdot g^{-1}$ at 0.21 $mA \cdot cm^{-2}$ with a capacity retention of 87.7% after 200 cycles is achieved at a sulfur loading of 1.3 $mg \cdot cm^{-2}$.

In addition to the design and optimization of compounding methods for conductive carbon materials, S can be combined with some metallic or nonmetallic elements with high electronic/ionic

conductivity, such as, sulfur-rich SeS_x [63], P_2S_{5+x} [64] and metal sulfides [65] to enhance the electrochemical kinetics. The specific studies of metal sulfides are described in detail in Section 3.3.

3.1.2. Triple-phase interfaces construction

Due to the intrinsic insulating properties of S, in the ASSLSBs cathode, a triple-phase interface needs to be constructed to ensure the electrochemical activity of S, but this greatly increases the proportion of inactive components in the composite cathode. Therefore, many researches have been conducted to enhance the effective quantity of the triple-phase interfaces by rational design of carbon materials and improving the material compounding method, thus reducing the proportion of inactive materials.

Porous carbon plays an important role in improving the electronic conductance of S. However, in solid-state systems, since SSEs cannot access S confined in deep pores, many carbon materials that are widely used in liquid systems do not perform well in solid-state systems, and porous carbon materials suitable for solid-state systems need to be rational designed. Sun et al. [66] prepared a N-doped carbon fiber with micropores located only at the surface with an ultrahigh surface area of 1519 $m^2 \cdot g^{-1}$. Since the porous layer exists only at the surface, the S loaded in the pores can effectively contact the SSEs, while the dense pores can improve the electronic conductivity. Therefore, the prepared carbon fiber can effectively improve the electronic conductivity, promote the reaction kinetics, thus improve the utilization of sulfur. The assembled ASSLSBs show an initial discharge capacity of 1166 $mAh \cdot g^{-1}$ at 0.05C and a specific capacity of 710 $mAh \cdot g^{-1}$ remains after 220 cycles at 0.1C (Fig. 5(A)).

Wang et al. [67] prepared a mixed ionic/electronic conductive LLTO/carbon nanofibers as the carrier for S, which effectively enlarged the active surface, improved the charge transfer efficiency, and promoted the electrochemical reaction of S. At the same time, due to the construction of effective interfaces, the proportion of inactive components can be effectively reduced, and the energy density of the battery can be improved (Fig. 5(B)).

There are also a few studies showing that composite cathodes containing only sulfur and conductive carbon materials can also achieve excellent electrochemical performance. Sakuda et al. [68] prepared mesoporous carbon materials with a large number of interconnected 5 nm mesopores and composited S with carbon matrix by melt diffusion method. The mesoporous carbon provides a great accommodation space and interconnected conductive paths for S, which effectively improves the utilization of S. The ASSLSBs can maintain a high specific capacity of nearly 1100 $mAh \cdot g^{-1}$ after 400 cycles at a current density of 1.3 $mA \cdot cm^{-2}$ (Fig. 5(C)).

3.1.3. Composite cathode optimization

The simple mixing of active materials, ionic-conducting phase and electronic-conducting phase in the composite cathode leads to tortuous ion and electron transport channels in the composite cathode, resulting in poor rate performance. Therefore, it is necessary to optimize the microstructure of the composite cathode and the volume fraction of each component. By systematically studying the sulfur-carbon black-Li_6PS_5Cl composite cathode, Dewald et al. [69] quantified the effect of the composite cathode on Li^+/e^- transport by changing the volume fractions of SSEs and carbon black. The authors employ tortuosity factors to describe Li^+/e^- transport in composite cathodes, and propose that the ionic conductivity of the SSEs is not equal to the effective ionic conductivity of the composite cathode, and the actual ionic conductivity of the composite cathode needs to be evaluated (Fig. 5(D)).

3.2. Lithium sulfide as active materials

As the fully-lithiated form of S, Li_2S can deliver a high theoretical specific capacity of 1166 $mAh \cdot g^{-1}$ and a high energy density of 1550 $Wh \cdot kg^{-1}$. Compared with the S that must be used with lithiated anode, Li_2S can be used with lithium-free and high specific energy anodes such as Si, so that it has wider applicability [70]. In addition, since the Li_2S undergoes a delithiation process firstly during charging, there will be no significant volume expansion on the cathode side, thereby increasing the mechanical stability of the composite cathode. Furthermore, since the melting point of Li_2S is much higher than that of S (938 °C vs. 112.8 °C), the preparation of materials can be carried out at higher temperature, thus broadening the processing schemes. However, it cannot be ignored that Li_2S, like S, has low ionic and electronic conductivities, resulting in a high activation barrier, and the high charge overpotential will result in the oxidation of the electrolyte, which leads to an increase in interfacial resistance.

3.2.1. Strategies of improving kinetics

The intrinsic ionic conductivity of Li_2S can be improved by doping, i.e., doping high-valent cation ions [71] at the Li site or halide ions at the S site. The Li^+ conductivity is improved due to vacancy

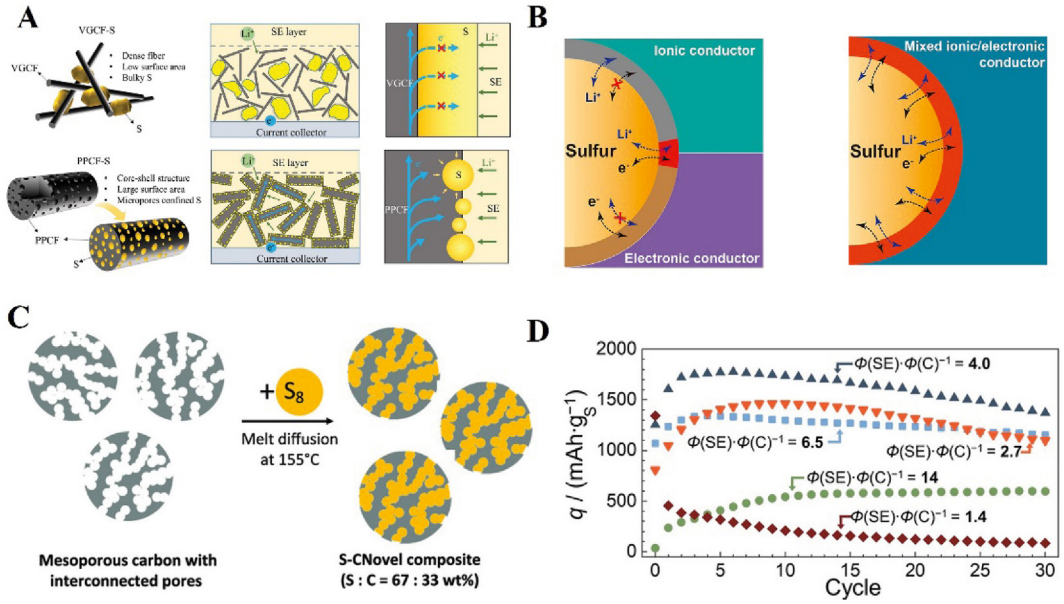

Fig. 5. (A) Schematic illustration of the structural effect of carbon additive in the cathode [66]. (B) Illustration of the charge-transfer behavior at traditional triple-phase interface and mixed ionically/electronically conductive double-phase interface [67]. (C) Schematic diagram of S—C Novel composite preparation [68]. (D) Cycling data for In/InLi|Li_6PS_5Cl|S-C-Li_6PS_5Cl SSB cells with various SE to carbon volume ratios ($\varphi(SE)\cdot\varphi(C)^{-1}$) in the composite cathode [69]. Copyright with 2021 Wiley-VCH GmbH, Copyright with 2022 American Chemical Society and Copyright with 2019 WILEY-VCH Verlag GmbH & Co. KGaA, Weinheim.

formation and the nano-ionic effect [72]. Gamo et al. [71] doped Li_2S with AlI_3 by mechanical ball milling which increases the room temperature ionic conductivity to 6×10^{-5} S·cm^{-1}. Wan et al. [73] showed by density functional theory (DFT) calculations that adding LiBr or LiI to Li_2S promotes the formation of vacancy defects (Fig. 6(A)), thereby improving the ionic conductivity.

In addition, the methods of decreasing the particle size and constructing effective conductive network can be adopted to reduce the charge and discharge overpotentials of Li_2S. Jiang et al. [74] synthesized Li_2S/CNT (47:53 in weight) by a liquid-phase composite method, in which Li_2S nanoparticles with a size of only 15 nm are anchored on the CNT, suppressing the secondary aggregation. The electronically conductive network provided by the continuous CNT matrix greatly enhances the electron transport at the interface. While the softer network relieves the stress generated during cycling, and the ion diffusion coefficient is increased by 39 times compared with the initial Li_2S (Fig. 6(B)), the overpotential between the charge—discharge platform is only around 0.3 V, achieving a high utilization rate of Li_2S. Han et al. [60] utilized a bottom-up method, i.e., co-precipitation and high-temperature carbonization by dispersing Li_2S, Li_6PS_5Cl and PVP in ethanol to construct a uniform three-phase interface (Fig. 6(C)). A high reversible capacity of 830 mAh·g^{-1} can be maintained for the Li-In|Li_6PS_5Cl|Li_2S-Li_6PS_5Cl-C cell after 60 cycles at a current density of 50 mA·g^{-1} with a Li_2S loading of 3.6 mg·cm^{-2}.

As far as carbon materials are concerned, the morphology and compounding methods play an important role [75]. Through a simple pyrolysis deposition approach, Wang et al. [76] coated Li_2S with a 20 nm N-doped carbon coating layer, which effectively reduces the dissociation activation energy of Li_2S and enhances the conversion kinetics. The ratio of Li_2S utilization is as high as 91% with a high Li_2S loading of 8.2 mg·cm^{-2} at 60 °C (Fig. 6(D)).

When Li_2S is used in SPEs, the intrinsic challenge of shuttle effect still exists. It is necessary to design functional structures to adsorb, encapsulate or catalyze LiPSs. Gao et al. [77] constructed Li_2S@TiS_2 particles with a core-shell structure by using the nanoscale encapsulation method. The 20 nm thick TiS_2 shell on the one hand inhibits the shuttle of LiPSs in the poly (ethylene oxide)-based electrolyte through adsorption, and on the other hand catalyzes the conversion of Li_2S to S. Liu et al. [70] designed the Li_2S@Co-C@MHF structure by coaxial electrospinning technique. Due to the strong interaction of the Co surface, the Li—S bond in Li_2S is weakened during the initial charging process, and the hollow MXene structure well encapsulates LiPSs through Lewis acid-base interaction and provides continuous electron transport channels, and LiPSs is converted to S through a flatter plateau at 2.33—2.34 V.

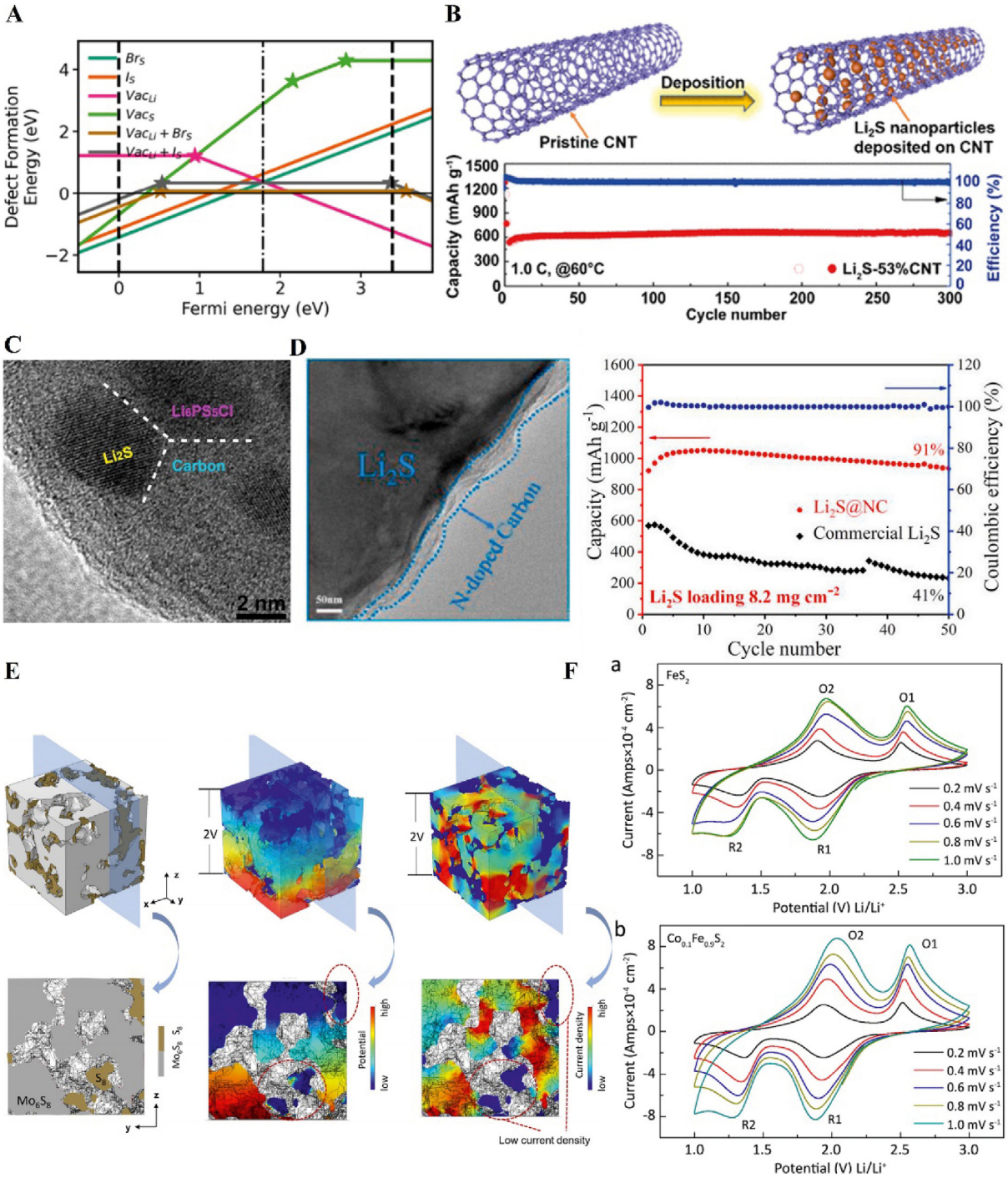

Fig. 6. (A) DFT calculations of the Li_2S-I-Br system [73]. (B) Schematic diagram of the Li_2S-CNT cathode and cycling stability of the Li_2S-53% CNT cathode under 1C at 60 °C [74]. (C) The high-resolution TEM image of the as-obtained Li_2S-Li_6PS_5Cl-C nanocomposite [60]. (D) TEM image of the as-obtained Li_2S@NC composite and comparison of the cycling performance (Li_2S@NC and commercial Li_2S) under Li_2S loading of 8.2 mg·cm^{-2} [76]. (E) 3D characterization, potential distribution and current density distribution of the Mo_6S_8/S cathode based on X-ray computed tomography (CT) data [81]. (F) CV curves of (a) FeS_2 and (b) $Co_{0.1}Fe_{0.9}S_2$ at different scan rates from 0.2 mV·s^{-1} to 1.0 mV·s^{-1} at the 2nd cycle [82]. Copyright with 2021 American Chemical Society, Copyright with 2016 American Chemical Society, Copyright with 2021 American Chemical Society, Copyright with 2022 American Chemical Society, Copyright with 2020 Elsevier B.V. and Copyright with 2019 American Chemical Society.

3.2.2. *Strategies of improving processability*

Finally, it cannot be ignored that the major bottleneck of Li_2S is its poor air stability, which impels Li_2S to be synthesized in an anhydrous and oxygen-free environment. In addition, the low solubility of Li_2S in organic solvents further limits its industrial application. The main method currently used is the recrystallization method, but this method is difficult to

obtain nanoparticles with uniform particle size. In contrast, the particle size prepared by the *in-situ* synthesis method is smaller and more uniform, which is mainly divided into chemical-synthesis method and electrochemical-conversion method. Yan et al. [78] adopted an ingenious one-step combustion method, i.e., burning CS_2 and Li metal to *in-situ* generate Li_2S@C, in which Li_2S nanocrystals are uniformly embedded in the conductive matrix. Benefiting from this unique architecture, the Li_2S@C composite cathode can achieve ultra-high Li_2S areal loading (7 $mg \cdot cm^{-2}$) and 91% Li_2S utilization. Apart from this, Jiang et al. [79] directly reduced Li_2SO_4 to Li_2S by the carbothermic method in the carbon-coated situation to construct a high electronic conductive channel. In the system, Li_2S can deliver a specific capacity as high as 1044.3 $mAh \cdot g^{-1}$ at a current density of 0.4 $mA \cdot cm^{-2}$ and a high loading of 6.03 $mAh \cdot cm^{-2}$. However, whether these chemical methods can be achieved on a large scale and environment friendly still needs further explorations [80].

Electrochemical methods refer to the methods that utilize deep discharge of some metal sulfides to generate metal nanoparticles and Li_2S, which will be explained in the next section.

3.3. Metal sulfides as active materials

Compared with sulfur, metal sulfide (MS) has higher electron and ion conductivities, which can change the point contact of triple-phase to surface contact, thus shortening the charge transport distance [83]. Secondly, the metal atoms generated after discharge process can reduce the polarization during cycling. More importantly, there are a large number of available metal sulfide minerals in nature to acquire easily [84,85]. Li et al. [81] designed an all-electrochem-active cathode (Mo_6S_8-S) without additional carbon and electrolyte, in which Mo_6S_8 can be rapidly charged and discharged based on the intercalation reaction while S delivers higher capacity based on conversion reaction. The distributions of potential, current and reaction hot spot in the electrode are relatively uniform. Thus, the battery shows a relatively low overpotential (Fig. 6(E)) and delivers an initial specific capacity of 1160 $mAh \cdot g^{-1}$ under a high load of 4.2 $mg \cdot cm^{-2}$.

3.3.1. Strategies of improving kinetics

The intrinsic kinetics of metal sulfides can be further modified, such as reducing particle size [86] or exfoliating layered sulfides, in which the diffusion paths of ions in the exfoliated nanosheets are reduced and the total interfacial contact area is increased [87]. In addition, doping on the metal sulfides is also a promising choice. Wan et al. [82] conducted a series of doping experiments for FeS_2, including $Co_{0.1}Fe_{0.9}S_2$, $Ni_{0.1}Fe_{0.9}S_2$ and $Cu_{0.1}Fe_{0.9}S_2$. Among them, the specific surface area of the Co-doped sample increased, and the catalytic effect of Co resulted in the surface-controlled pseudocapacitance, which shortened the ion transport path and improved the rate capability.

3.3.2. Macrostructure design

For MS undergoing conversion reaction, since its own structure is destroyed when it converts into metal atom and Li_2S, it is also important to build a conductive network in the electrode. Yamakawa et al. [88] firstly found that Cu^+ has high mobility in LiCuS, resulting in the formation of larger Cu particles at the end of the discharge process. Santhosha et al. [84] took advantage of this property by utilizing CuS self-reduction to form a micrometer-sized and well-crystallized conductive network. In addition, for reaction with a large volume change, the addition of carbon can buffer the volume change during the charge-discharge process, and the CuSC(3−2) with the addition of a conductive agent exhibits a coulombic efficiency of 99.9% even after 800 cycles [89].

Up to now, there has been a lot of research on the application of various metal sulfides in solid-state batteries, but at this stage it is still difficult to realize high energy density, high-rate performance and high stability simultaneously. In the future, more structural and functional designs are needed for the development of ASSLSBs using metal sulfides.

4. Anode materials

4.1. Lithium metal

Lithium metal is considered the "holy grail" of the anode materials of the lithium batteries due to its lowest chemical potential (−3.04 V vs. SHE), low density (0.59 $g \cdot cm^{-3}$) and ultra-high specific capacity (3860 $mAh \cdot g^{-1}$). However, due to the high reactivity of lithium metal, many electrolytes with high ionic conductivity such as $Li_{10}GeP_2S_{12}$ (LGPS) are reduced, causing severe side reactions at the anode/electrolyte interface, and depletion of lithium metal and electrolyte. The infinite volume change during cycling and the uneven deposition of lithium at the interface will cause the rupture of SEI and the growth of lithium dendrites, which will result in the continuous consumption of lithium during cycling, and lead to the generation of "dead lithium" and the pulverization of electrodes. The current main strategies are to use lithium alloy and/or perform interfacial modification.

4.2. Li-M alloys

Li-M alloys (M = Al, In, Si, B) are chosen as alternatively anodes to avoid Li dendrites and alleviate the side reactions. Usually, the Li^+ diffusion coefficients of Li-M alloys are higher than those of Li metals, so that faster Li^+ channels can be constructed in the bulk phase. In addition, the potentials of Li-M alloys are often 0.3−0.6 V higher than that of lithium metal, thus enhance the affinity for lithium ions and reduce the driving force for reducing electrolytes thermodynamically, and it can effectively inhibit the formation of lithium dendrites and stabilize the anode/electrolyte interface.

Due to its constant redox potential (0.62 V vs. Li^+/Li) over a wide stoichiometric range (0−45% at %), good chemical/electrochemical stability and mechanical ductility, Li-In alloy is the most widely used lithium alloy anode in the laboratory (Fig. 7(A)) [90]. Hou et al. [62] successfully prepared an ASSLSB composed of Li-In alloy anode, LGPS electrolyte, and S@CNT cathode. However, the lower theoretical specific capacity (233 $mAh \cdot g^{-1}$) and higher electrode potential greatly reduce the energy density of the full cell, limiting its application in high energy density ASSLSBs systems.

In response to this problem, Zeng et al. [90] proposed that Al has high electronic conductivity (3.5×10^7 $S \cdot m^{-1}$), excellent ductility, and high specific capacity (990 $mAh \cdot g^{-1}$), which can be an promising high performance anode candidate for ASSLSBs. The $Li_{0.8}Al$ anodes can be prepared without using binders and conductive carbon additives. The ASSLSBs composed of $Li_{0.8}Al$ alloy anode and melting-coated S composite cathode operate steadily for over 200 cycles with a capacity retention of 93.29%.

Si has also received a lot of attention from researchers because of its ultra-high theoretical specific capacity of 4200 $mAh \cdot g^{-1}$ when fully alloyed. Meng et al. [91] prepared a high-purity micron silicon cathode without the addition of conductive carbon, which alleviates the degradation of sulfide electrolytes by forming a stable SEI due to the absence of conductive carbon. The voids created by the volume change of the Li-Si alloy anode during alloying and dealloying can be reduced by the applied pressure, thus maintaining good contact.

The lower atomic mass of boron makes the Li-B alloys have lower density, and the reaction of B with a large amount of lithium to form Li-rich phase Li-B alloys leads to lower electrochemical potential (ca. 0.05 V vs. Li^+/Li), which ensures the high discharge voltage and mass energy density of the assembled battery. At the same time, the unique 3D skeleton structure of the Li-B alloys allow it to induce uniform lithium deposition during the lithium platting/stripping process, reducing the volume expansion during cycling and maintaining the integrity of the electrode. Chen et al. [92] incorporating the Li-B (80LiB) alloy with a unique 3D skeleton and Ag@C modified layer to achieve bulk phase/interface synergistic effect, thus effectively mitigating the volume change during cycling, inducing uniform platting/stripping of Li, maintaining the electrode integrity and inhibiting the growth of Li dendrites, and suppressing the occurrence of interfacial side reactions. The assembled ASSLSBs deliver a specific capacity of 1316 $mAh \cdot g^{-1}$ and a capacity retention of 82% after 60 cycles (Fig. 7(B)).

5. Interface engineering

Compared with traditional liquid Li-S batteries based, the main challenge faced by ASSLSB is the poor solid-solid contact between electrode and electrolyte. In response to this problem, researchers have developed various methods to provide fast ion channels and reduce interfacial resistance.

5.1. Cathode/electrolyte interface

Due to the adoption of composite strategies, complex composition at the cathode side will result in more complicated interface interactions. The large volume change of sulfur upon cycling can cause contact losses in the composite, which can hinder reversible redox transformations of active materials as due to the degradation of the triple-phase interface. Other than mechanical failure, the interface is also of great importance in electrochemical failure. While a high interfacial contact area among composite cathodes is essential to fully utilize insulating active materials, the substantial interfacial area between solid electrolytes and carbon additives can cause non-negligible degradation of the electrolyte, which will dramatically deteriorate the cycling performance of the cell [96].

5.1.1. Mechanical compatibility

Point-to-point contact and continued volume expansion/contraction lead to increased interfacial ion transport resistance, resulting in charge inhomogeneity and anisotropic charge concentration, which may further cause accumulated intrinsic stress and microcracks on active particles [97], further deteriorating cycling performance. Dealing with the “chemo-mechanical failure”, the

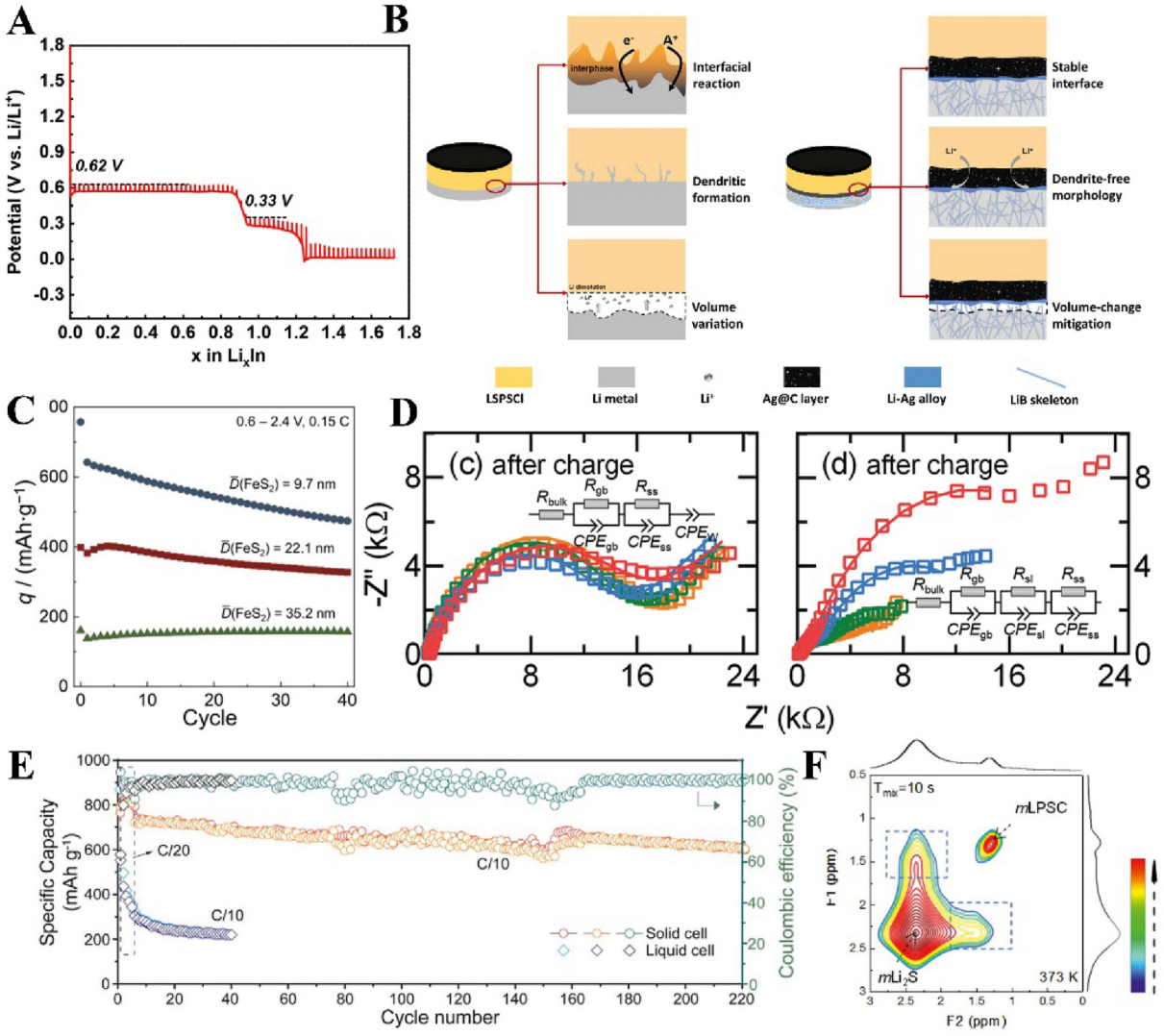

Fig. 7. (A) Galvanostatic intermittent titration technique profile of the lithiation process of the In foil [90]. (B) Schematic illustration of the problems when using a Li metal anode (left) and our proposed synergistic approaches of a Ag@C modified 80LiB alloy anode (right) [92]. (C) Influence of the FeS_2 particle size on cycling performance of In/InLi|Li_6PS_5Cl|FeS_2-C-Li_6PS_5Cl cells at 25 °C and an areal FeS_2 loading of 3.8 mg·cm^{-2} in the cathode composite [86]. (D) Nyquist plots of the bare solid-state Li_2S cell (left panels) and the Li_2S cell with the solvate interlayer (right panels) [93]. (E) Long-term cycling performance comparison between solid-state cell and liquid cell at the rate of C/10 of Li-In|$Li_{6.6}Ge_{0.6}Sb_{0.4}S_5I$|$FeS_2$+$Li_{6.6}Ge_{0.6}Sb_{0.4}S_5I$+C (4:5:1) [94]. (F) Two-dimensional ^{6}Li-^{6}Li exchange spectra for the mixture of micron-sized LPSC and Li_2S-LiI (3:1) cathodes measured at a spinning speed of 10 kHz and 373 K with a mixing time of 10 s [95]. Copyright with 2022 American Chemical Society, Copyright 2021 Angewandte Chemie International Edition published by Wiley-VCH GmbH, Copyright 2019 WILEY-VCH Verlag GmbH & Co. KGaA, Weinheim and Copyright 2020 Wiley-VCH GmbH.

in-situ liquid phase synthesis strategy is considered to be an appropriate method to improve the contact between solid electrolyte and active material particles, i.e., dissolving SE or its precursor in a compatible solution, and directly *in-situ* compositing on the surface of active particles by dissolution-deposition or heat treatment method [98−100]. Yao et al. constructed $Li_7P_3S_{11}$ crystalline electrolyte particles with ionic conductivity as high as 1.5×10^{-3} S·cm^{-1} on Co_9S_8 by this method [65], which effectively provides tight interfacial contact, thereby reducing the interfacial resistance and stress-strain during cycling [101]. In addition, the *in-situ* formed thin electrolyte layer avoids the application of excess electrolyte, which improves the energy density of the battery dramatically. Furthermore, this mild method has the opportunity to achieve one-step synthesis from electrolyte precursors to composite electrodes, which is critical to simplify industrial manufacturing processes [102].

As mentioned above, even though a lot of works have been done to enhance the poor solid-solid contact, the polarization problem in the solid-

state system is still far greater than that in the LE. In consideration of this circumstance, moderate compatible LE can be added directly on the electrode side to improve the interfacial contact. In this kind of work, the compatibility of the electrolyte with SE should be considered firstly, especially for sulfides that are easily attacked by polar nucleophilic solvents. In recent years, high-concentration electrolyte is usually used by researchers to improve interfacial stability due to the reduction in the proportion of free polar solvents. Cao et al. [103] proposed a high-concentration LiTFSI in triglyme at molar ratio of 1:1 to stabilize the cathode/$Li_{10}GeP_2S_{12}$ electrolyte interfaces and demonstrated its application in a ASSLSB. In this system, Li salts are more coordinated, thereby reducing the nucleophilicity of ether oxygens. Furthermore, Shin et al. [93] introduced a local high-concentration system $(MeCN)_2$-LiTFSI:TTE into the interfacial layer of SSLSB, and the interfacial resistance of the system modified by the interlayer gradually decreased during cycling (Fig. 7(D)).

5.1.2. Electrochemical compatibility

Besides mechanical compatibility, the electrochemical compatibility between active material and electrolyte in composite cathodes is also important. Non-equilibrium carrier transport at the interface is determining [104,105]. Bulk carrier transport is sluggish due to the isolated property of sulfur itself, leading to the unequilibrium of local ionic concentration gradient, electric fields and resulting uneven reaction. Besides, compared with the oxide cathodes used commonly, the oxidation potential of sulfur and sulfide is lower. Although no violent interfacial reaction will occur, the limited interfacial reaction can also lead to hindered Li^+ interfacial transport, resulting in an increase in polarization. Especially for the sulfide SSE, the upper limit of electrochemical window of which is close to the oxidation potential of active materials, so providing fast ion transport channels while minimizing electrolyte degradation at the interface should be also taken into consideration. For example, Dewald et al. [86] prepared a higher specific surface area of FeS_2 by reducing the particle size to 9.7 nm, which effectively enhances the electrochemical performance. However, it shouldn't be ignored that the capacity degradation was more drastic, which is attributed to the severe interfacial degradation owing to lager specific surface area (Fig. 7(C)). To mitigate the degradation of the interface, Sun et al. [94] fine-tuned the operating voltage range of FeS_2 according to the electrochemical window of $Li_{6.6}Ge_{0.6}Sb_{0.4}S_5I$, thereby realizing a 84.5% capacity retention after 220 cycles (Fig. 7(E)). The only disadvantage of adopting this strategy is that it may not be able to fully utilize the capacity of the active material.

In this dilemma, the interfacial buffer layers can be constructed by strategies of interfacial modification [47]. An effective strategy is to introduce lithium salts that have suitable ionic conductivity and are more resistant to oxidation. Liu et al. [95] used 2D exchange spectroscopy (2D-EXSY) to quantify the lithium ion diffusion at the interface. It showed that there was almost no exchange between Li_2S and Li_6PS_5Cl (LPSC) after a mixing time of 20 s, indicating poor Li^+ diffusion between the two phases. However, in the phase between Li_2S and LPSC coated with LiI, even if the mixing time is only 10 s, an obvious off-diagonal exchange peak is found, which indicates that the presence of LiI reduces the interface degradation between Li_2S and LPSC, and guarantees fast Li^+ transport at the interface (Fig. 7(F)). However, the uses of a large amount of LiI and LiBr that do not contribute to the capacity will reduce the energy density of the electrode. In response to this, Takashi Hakari et al. [106] proposed a hierarchical adjustment strategy. First, Li_2S and C were mixed with a small amount of Li_3PO_4 and Li_2SO_4 by ball milling to form uniform primary particles. Among them, Li_3PO_4 has moderate ionic conductivity and high oxidation resistance while the addition of Li_2SO_4 improves the ionic conductivity further, thereby constructing an interface with high compatibility and fast kinetics. The full cell can achieve a high energy density of over 500 $Wh \cdot kg^{-1}$ (considering the total weight of the SE layer, Li metal and current collectors) for several cycles at 60 °C and a current density of 116.7 $mA \cdot g^{-1}$.

5.2. Anode/electrolyte interface

The above-mentioned work is basically based on the modification of the cathode/solid electrolyte interfaces, but the stability of the anode/solid electrolyte interface is also a major factor for the stable cycling of the lithium-sulfur battery. Especially in the solid-state field, the chemical and mechanical compatibility of the interface between the anode and SSEs needs to be considered in a more systematic way. The main issues that need to be addressed on the anode side are the compatibility of the solid-state electrolyte with the lithium metal anode and the growth of lithium dendrites. At present, the commonly used strategies include the application of electrolytes that can form stable SEI layers with lithium metal anode, interfacial modification and the application of lithium alloy anodes.

The root cause of the instability of the electrolyte to lithium metal is that, as soon as the electrolyte is

in contact with lithium metal, it will react continuously when the by-products can conduct both electrons and ions, so that the lithium metal is continuously consumed and the SEI is continuously thicken. This results in the gradually increasing in the interface impedance and the cell polarization, which eventually leads to the failure of the battery. Currently, no electrolytes that are intrinsically stable to Li metal have been reported, but many electrolytes that can form stable SEI with Li metal have been extensively studied, such as $LiBH_4$-based electrolytes [107], Li_3PS_4 and $0.75Li_2S$-$0.24P_2S_5$-$0.1P_2O_5$. In a Li-Li symmetric cell with $0.7Li(CB_9H_{10})$-$0.3Li(CB_{11}H_{12})$ electrolyte, the plating/stripping overpotential is essentially unchanged at a current density of 0.2 $mA \cdot cm^{-2}$ for 300 cycles (Fig. 8(A)). Considering the stability of composite hydride-based electrolytes against Li metal, Kisu et al. [108] proposed that the problem of fast capacity decay can be attributed to the degradation of the cathode/electrolyte interface. Cross-sectional scanning electron microscopic observation showed that cracks appeared in the cathode region during cycling, and the cathode thickness continued to be increased. Raman spectra and XRD patterns indicated that the $Li_4(BH_4)_3I$ electrolyte continued to be decomposed during cycling, thus causing the problem of fast capacity decay.

In addition, interfacial modification can also be performed at the anode interface to improve the interfacial compatibility, which requires precise design according to the type of electrolyte. For the interface between the lithium metal anode and some inorganic SSEs with high rigidity, the interfacial buffer layer can improve the solid-solid contact of the interface [109]. Bosubabu et al. [110] introduced a polypropylene (PP) wetting layer at the interface between LAGP and lithium metal, which reduced the interface resistance and polarization, and the charge transfer resistance was much smaller than that of the system without the introduction of the interface layer (Fig. 8(B)). For the interface between lithium metal and polymer-based electrolytes, Judez et al. [111] used atomic layer deposition technology to deposit Al_2O_3 with a thickness of 5 nm on the negative side of the electrolyte, which significantly improves the stability of PEO-based electrolytes against lithium metal while suppressing the side reactions of LiPSs and Li.

Due to the nonuniformity in ionic conductivity of the solid electrolytes, the uneven deposition of Li at the interface results in the growth of lithium dendrites. Yin et al. [112] improved the thermal uniformity of the electrolyte by adding 2D BN nanosheets to the PEO-based electrolyte, which helps achieve uniform current density distribution on the interface, and effectively promote the uniform deposition of Li and the homogeneous conversion reactions in the cathode (Fig. 8(C)).

The above work is to improve the interfacial compatibility by introducing the modification layer, which will increase the difficulty and cost of preparation in practical applications. Therefore, some methods of *in-situ* generating stable SEI can be adopted to simplify the process of constructing the modification layer and achieve closer interfacial contact [42,113]. Li et al. [114] used azo compounds as PEO electrolyte additives, and utilized the free radicals generated by the decomposition of azo salts with different electron densities and diffused to the electrode surface to *in-situ* build a stable and uniform interfacial layer. In the presence of high electron density benzene rings, the additionally generated Li_3N will further enhance the interfacial stability.

6. Summary and outlooks

We have outlined the major SSLSB battery types and the advancements made. It can be seen that ASSLSBs have the potential to achieve a high energy density of 500 $Wh \cdot kg^{-1}$, low self-discharge, long-term cycling stability and high safety. However, the practical application of ASSLSB is still a long way off, which rely upon the research and development of sulfur composite cathodes with both high S content ($\geq$50 wt%) and high areal S mass loading ($\geq$5 $mg \cdot cm^{-2}$), large scale preparation of electrode/electrolyte materials and practical electrode/electrolyte membranes, and the rational design of the electrode/electrolyte interfaces.

In terms of the cathode, it mainly relies on the construction of the triple-phase percolated conduction network for both Li^+ and electron transportation within ionic conductive phase, electronic conductive phase and active materials to fully utilize the insulating active materials. Therefore, further improving the ionic conductivity of the SE and the electronic conductivity of the conductive agent are of great significance. Among them, the incorporation of small amounts of doping elements is an important and feasible way to promote the carrier transport. The composite cathode of sulfur and metal sulfides with high specific capacity should be further explored to achieve desirable electrochemical performance, especially on the catalytic mechanism and structure-properties relationship.

Further, the design and fabrication of advanced large-scale practical sulfur cathode still remains a

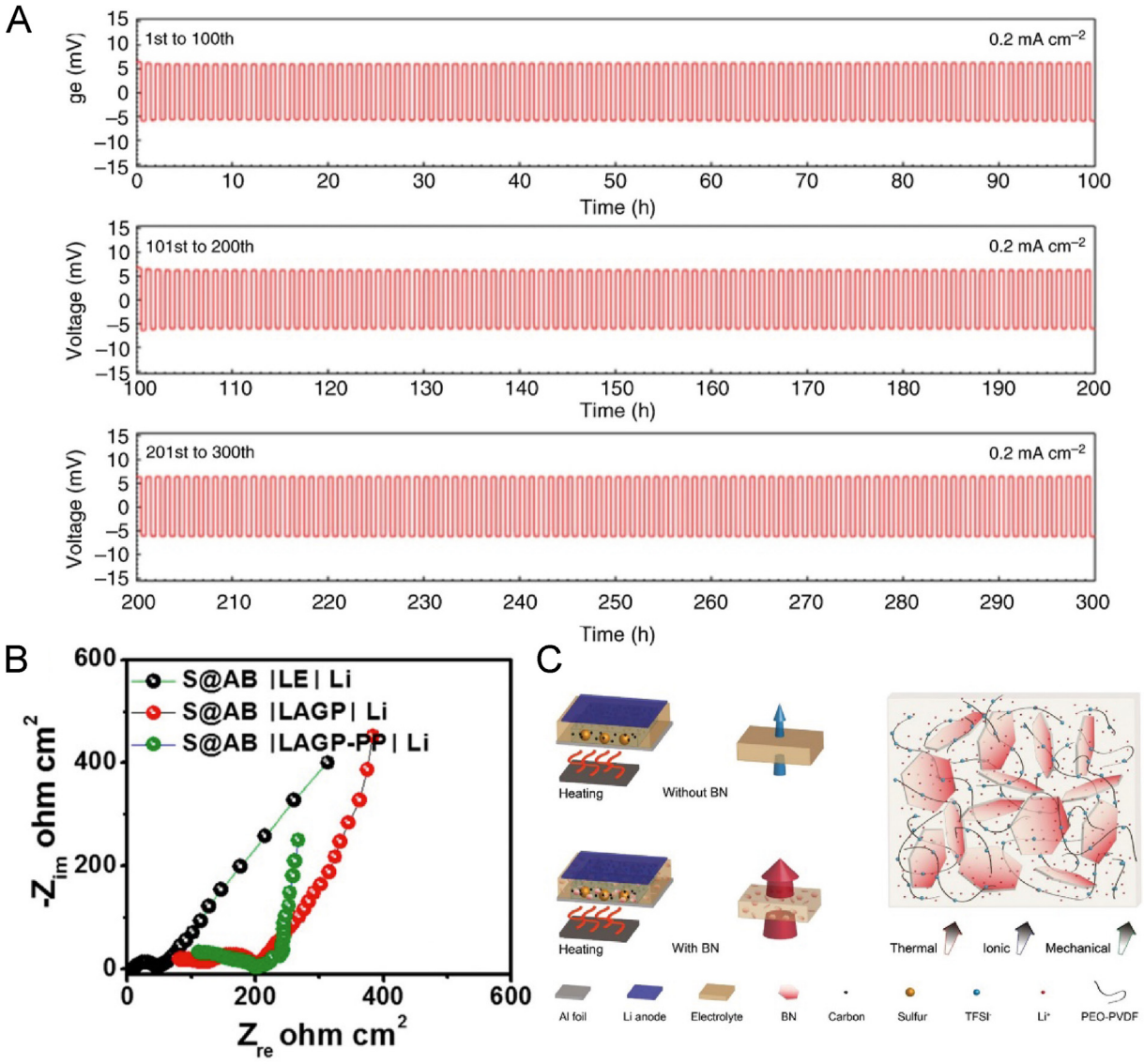

Fig. 8. (A) Galvanostatic cycling profiles for prolonged cycles [107]; (B) Nyquist plots of S@AB|LE|Li, S@AB|LAGP|Li, and S@AB|LAGP-PP|Li cells [110]; (C) Rational design of solid-state polymer electrolyte with BN additive [112]. Copyright with 2019 American Chemical Society.

key challenge. The emerging dry electrode technology can be an attractive and effective technique for addressing this challenge. As for the carrier transport property of thick electrode, tortuous carrier transport paths should be minimized, so it is necessary to develop a novel structure design for the composite cathode based on material properties to reduce the tortuosity, other than the commonly-used mechanical grinding. Well-compositing process based on liquid and gas phase-based techniques should also be developed and optimized to achieve intimate contact between the components. At the same time, in order to evaluate the performance and unravel the structure-performance relationships of composite cathodes in more detail, advanced techniques and new analytical methodologies are required for the quantification of the effective conductivity and operando monitoring of carrier transport.

The last point about cathode to be emphasized is that mold cells are widely used in current works with a high stack pressure applied during operation, which effectively mitigate the negative effects of the huge volume change. The high stack pressure requirement is a point of criticism for the practical application of ASSLSBs. The factors determining stack pressure and the engineering challenges at the module to cell-level design must be systematically investigated. During cycling, it is necessary to pay attention to the chemical, electrochemical and mechanical stabilities of the components of the cathode. These problems are often coupled with each other and then affect the whole cell. In response to these issues, exploring

electrolyte that will not degrade during processing and cycling, and building high stable interfacial structure are two promising directions.

As for electrolytes, the focus of improvements is to enhance the mechanical stability, processability, ionic conductivity and industry-scale production ability. Polymer-based and derived composite electrolytes can achieve high flexibility, suitable electrochemical window with thin membrane. However, the main challenges at present are the low ionic conductivity and the unavoidable shuttle effects of LiPSs. The development of single-ion conductors and the modification of local coordination by designing lithium salts are effective methodologies to further improve ionic conductivity. Adding inorganic fillers or designing functional groups to inhibit the shuttle effect of LiPSs are important strategies to improve the coulombic efficiency and inhibit the self-discharge effect.

It is worth noting that a lot of works on oxide-based composite electrolytes are still in the incipient stage, and there are few systematic studies on the trade-off between controlling the ratio of inorganic fillers to suppressing the shuttle effect and maintaining high ionic conductivity. At the same time, it is significant to carry on more in-depth research on ion transport pathway in composite solid electrolytes, especially for interfacial Li-ion transport along the nanofiller/polymer interface, which is of great importance to develop functionalized ceramic particle-based composite electrolytes with high ionic conductivity dominated by interfacial ion transport.

For sulfide electrolytes, the thick solid electrolyte separator is the major challenge. Flexible and thin-layer membrane (<50 μm) is necessary to fulfill the high energy density potential of ASSLSBs, which relies on wet technology or solvent-free dry-film process. Among them, the approaches of wet technology are still premised on the chemical stability of the sulfide electrolytes on solvents.

As regard to the anode side, a large number of the current works are based on Li-In alloy anodes to achieve high cycling stability. However, the low specific capacity of Li-In alloy anode significantly limits the energy densities of ASSLSBs. Also, Indium is a rare element and expensive, which restricts its practical application. In comparison, the use of lightweight lithium alloys such as Li-Al and Li-B is a promising strategy to address the lithium metal anode/electrolyte interfacial challenge and achieve promising high energy density. Considering of the energy density, Li metal is still the "holy grail", in which the use of *in-situ* interfacial modification strategies to construct stable Li/electrolyte interphase and suppress lithium dendrite formation can be promising approaches to achieve both high energy density and long-term cycling stability.

Acknowledgements

This work is financially supported by the National Natural Science Foundation of China (Grant no.21935009) and the National Key R&D Program of China (Grant No. 2021YFB2401800).

References

[1] Yang X F, Luo J, Sun X L. Towards high-performance solid-state Li-S batteries: from fundamental understanding to engineering design[J]. Chem. Soc. Rev., 2020, 49(7): 2140−2195.

[2] Umeshbabu E, Zheng B Z, Yang Y. Recent progress in all-solid-state lithium-sulfur batteries using high Li-ion conductive solid electrolytes[J]. Electrochem. Energy Rev., 2019, 2(2): 199−230.

[3] Wu J H, Shen L, Zhang Z H, Liu G Z, Wang Z Y, Zhou D, Wan H L, Xu X X, Yao X Y. All-solid-state lithium batteries with sulfide electrolytes and oxide cathodes[J]. Electrochem. Energy Rev., 2021, 4(1): 101−135.

[4] Wu J H, Liu S F, Han F D, Yao X Y, Wang C S. Lithium/sulfide all-solid-state batteries using sulfide electrolytes[J]. Adv. Mater., 2021, 33(6): 2000751.

[5] Ohno S, Zeier W G. Toward practical solid-state lithium-sulfur batteries: challenges and perspectives[J]. Acc. Mater. Res., 2021, 2(10): 869−880.

[6] Schlem R, Burmeister C F, Michalowski P, Ohno S, Dewald G F, Kwade A, Zeier W G. Energy storage materials for solid-state batteries: design by mechanochemistry [J]. Adv. Energy Mater., 2021, 11(30): 2101022.

[7] Li M Y, Liu T, Shi Z, Xue W J, Hu Y S, Li H, Huang X J, Li J, Suo L M, Chen L Q. Dense all-electrochem-active electrodes for all-solid-state lithium batteries[J]. Adv. Mater., 2021, 33(26): 2008723.

[8] Cai X M, Cui B W, Ye B, Wang W Q, Ding J L, Wang G C. Poly(ionic liquid)-based quasi-solid-state copolymer electrolytes for dynamic-reversible adsorption of lithium polysulfides in lithium-sulfur batteries[J]. ACS Appl. Mater. Interfaces, 2019, 11(41): 38136−38146.

[9] Guan X, Wu Q P, Zhang X W, Guo X H, Li C L, Xu J. *In-situ* crosslinked single ion gel polymer electrolyte with superior performances for lithium metal batteries[J]. Chem. Eng. J., 2020, 382: 122935.

[10] Mackanic D G, Michaels W, Lee M, Feng D W, Lopez J, Qin J, Cui Y, Bao Z N. Crosslinked poly(tetrahydrofuran) as a loosely coordinating polymer electrolyte[J]. Adv. Energy Mater., 2018, 8(25): 1800703.

[11] Judez X, Zhang H, Li C M, Eshetu G G, Zhang Y, Gonzalez-Marcos J A, Armand M, Rodriguez-Martinez L M. Polymer-rich composite electrolytes for all-solid-state Li-S cells[J]. J. Phys. Chem. Lett., 2017, 8(15): 3473−3477.

[12] Wang L L, Ye Y S, Chen N, Huang Y X, Li L, Wu F, Chen R J. Development and challenges of functional electrolytes for high-performance lithium-sulfur batteries [J]. Adv. Funct. Mater., 2018, 28(38): 1800919.

[13] Pan K C, Zhang L, Qian W W, Wu X K, Dong K, Zhang H T, Zhang S J. A flexible ceramic/polymer hybrid solid electrolyte for solid-state lithium metal batteries[J]. Adv. Mater., 2020, 32(17): 2000399.

[14] Dixit M B, Zaman W, Hortance N, Vujic S, Harkey B, Shen F Y, Tsai W Y, De Andrade V, Chen X C, Balke N, Hatzell K B. Nanoscale mapping of extrinsic interfaces in hybrid solid electrolytes[J]. Joule, 2020, 4(1): 207−221.

[15] Wang G L, Zhu X Y, Rashid A, Hu Z L, Sun P F, Zhang Q B, Zhang L. Organic polymeric filler-amorphized poly(ethylene oxide) electrolyte enables all-solid-state lithium-metal batteries operating at 35 °C[J]. J. Mater. Chem., 2020, 8(26): 13351−13363.

[16] Sheng O W, Jin C B, Luo J M, Yuan H D, Fang C, Huang H, Gan Y P, Zhang J, Xia Y, Liang C, Zhang W K, Tao X Y. Ionic conductivity promotion of polymer electrolyte with ionic liquid grafted oxides for all-solid-state lithium-sulfur batteries[J]. J. Mater. Chem., 2017, 5(25): 12934−12942.

[17] Cai X M, Ding J L, Chi Z Y, Wang W Q, Wang D Y, Wang G C. Rearrangement of ion transport path on nano-cross-linker for all-solid-state electrolyte with high room temperature ionic conductivity[J]. ACS Nano, 2021, 15(12): 20489−20503.

[18] Zhang H, Oteo U, Judez X, Eshetu G G, Martinez-Ibanez M, Carrasco J, Li C M, Armand M. Designer anion enabling solid-state lithium-sulfur batteries[J]. Joule, 2019, 3(7): 1689−1702.

[19] Wang Y, Ji H F, Zhang X J, Shi J J, Li X N, Jiang X X, Qu X W. Cyclopropenium cationic-based covalent organic polymer-enhanced poly(ethylene oxide) composite polymer electrolyte for all-solid-state Li-S battery[J]. ACS Appl. Mater. Interfaces, 2021, 13(14): 16469−16477.

[20] Marceau H, Kim C S, Paolella A, Ladouceur S, Lagace M, Chaker M, Vijh A, Guerfi A, Julien C M, Mauger A, Armand M, Hovington P, Zaghib K. Operando scanning electron microscopy and ultraviolet-visible spectroscopy studies of lithium/sulfur cells using all solid-state polymer electrolyte[J]. J. Power Sources, 2016, 319: 247−254.

[21] Song Y X, Shi Y, Wan J, Lang S Y, Hu X C, Yan H J, Liu B, Guo Y G, Wen R, Wan L J. Direct tracking of the polysulfide shuttling and interfacial evolution in all-solid-state lithium-sulfur batteries: a degradation mechanism study [J]. Energy Environ. Sci., 2019, 12(8): 2496−2506.

[22] Li X, Wang D H, Wang H C, Yan H F, Gong Z L, Yang Y. Poly(ethylene oxide)-$Li_{10}SnP_2S_{12}$ composite polymer electrolyte enables high-performance all-solid-state lithium sulfur battery[J]. ACS Appl. Mater. Interfaces, 2019, 11(25): 22745−22753.

[23] Bai Y, Zhao Y B, Li W D, Meng L H, Bai Y P, Chen G R. New insight for solid sulfide electrolytes LSiPSI by using Si/P/S as the raw materials and I doping[J]. ACS Sustain. Chem. Eng., 2019, 7(15): 12930−12937.

[24] Liu Y, Liu H W, Lin Y T, Zhao Y X, Yuan H, Su Y P, Zhang J F, Ren S Y, Fan H Y, Zhang Y G. Mechanistic investigation of polymer-based all-solid-state lithium/sulfur battery[J]. Adv. Funct. Mater., 2021, 31(41): 2104863.

[25] Gao X, Zheng X L, Tsao Y C, Zhang P, Xiao X, Ye Y S, Li J, Yang Y F, Xu R, Bao Z N, Cui Y. All-solid-state lithium-sulfur batteries enhanced by redox mediators[J]. J. Am. Chem. Soc., 2021, 143(43): 18188−18195.

[26] Ji Y C, Yang K, Liu M Q, Chen S M, Liu X H, Yang B, Wang Z J, Huang W Y, Song Z B, Xue S D, Fu Y D, Yang L Y, Miller T S, Pan F. PIM-1 as a multifunctional framework to enable high-performance solid-state lithium-sulfur batteries[J]. Adv. Funct. Mater., 2021, 31(47): 2104830.

[27] Kim K J, Balaish M, Wadaguchi M, Kong L P, Rupp J LM. Solid-state Li-metal batteries: challenges and horizons of oxide and sulfide solid electrolytes and their interfaces[J]. Adv. Energy Mater., 2021, 11(1): 2002689.

[28] AbdelHamid A A, Cheong J L, Ying J Y. $Li_7La_3Zr_2O_{12}$ sheet-based framework for high-performance lithium-sulfur hybrid quasi-solid battery[J]. Nano Energy, 2020, 71: 104633.

[29] Yu X W, Liu Y J, Goodenough J B, Manthiram A. Rationally designed PEGDA-LLZTO composite electrolyte for solid-state lithium batteries[J]. ACS Appl. Mater. Interfaces, 2021, 13(26): 30703−30711.

[30] Bag S, Zhou C, Kim P J, Pol V G, Thangadurai V. LiF modified stable flexible PVDF-garnet hybrid electrolyte for high performance all-solid-state Li-S batteries[J]. Energy Storage Mater., 2020, 24: 198−207.

[31] Li W W, Sun C Z, Jin J, Li Y P, Chen C H, Wen Z Y. Realization of the Li^+ domain diffusion effect via constructing molecular brushes on the LLZTO surface and its application in all-solid-state lithium batteries[J]. J. Mater. Chem., 2019, 7(48): 27304−27312.

[32] Yan C Y, Zhou Y, Cheng H, Orenstein R, Zhu P, Yildiz O, Bradford P, Jur J, Wu N Q, Dirican M, Zhang X W. Interconnected cathode-electrolyte double-layer enabling continuous Li-ion conduction throughout solid-state Li-S battery[J]. Energy Storage Mater., 2022, 44: 136−144.

[33] Kou W J, Wang J X, Li W P, Lv R X, Peng N, Wu W J, Wang J T. Asymmetry-structure electrolyte with rapid Li^+ transfer pathway towards high-performance all-solid-state lithium-sulfur battery[J]. J. Membr. Sci., 2021, 634: 119432.

[34] Liu Z C, Fu W J, Payzant E A, Yu X, Wu Z L, Dudney N J, Kiggans J, Hong K L, Rondinone A J, Liang C D. Anomalous high ionic conductivity of nanoporous β-Li_3PS_4[J]. J. Am. Chem. Soc., 2013, 135(3): 975−978.

[35] Mizuno F, Hayashi A, Tadanaga K, Tatsumisago M. New, highly ion-conductive crystals precipitated from Li_2S-P_2S_5 glasses[J]. Adv. Mater., 2005, 17(7): 918−921.

[36] Seino Y, Ota T, Takada K, Hayashi A, Tatsumisago M. A sulphide lithium super ion conductor is superior to liquid ion conductors for use in rechargeable batteries[J]. Energy Environ. Sci., 2014, 7(2): 627−631.

[37] Kanno R, Maruyama M. Lithium ionic conductor thio-LISICON: the Li_2S-GeS_2-P_2S_5 system[J]. J. Electrochem. Soc., 2001, 148(7): A742−A746.

[38] Ong S P, Mo Y F, Richards W D, Miara L, Lee H S, Ceder G. Phase stability, electrochemical stability and ionic conductivity of the $Li_{10\pm1}MP_2X_{12}$ (M = Ge, Si, Sn, Al or P, and X = O, S or Se) family of superionic conductors [J]. Energy Environ. Sci., 2013, 6(1): 148−156.

[39] Boulineau S, Courty M, Tarascon J M, Viallet V. Mechanochemical synthesis of Li-argyrodite Li_6PS_5X (X = Cl, Br, I) as sulfur-based solid electrolytes for all solid state batteries application [J]. Solid State Ion., 2012, 221: 1−5.

[40] Chen S R, Niu C J, Lee H, Li Q Y, Yu L, Xu W, Zhang J G, Dufek E J, Whittingham M S, Meng S, Xiao J, Liu J. Critical parameters for evaluating coin cells and pouch cells of rechargeable Li-metal batteries[J]. Joule, 2019, 3(4): 1094−1105.

[41] Liang J W, Chen N, Li X N, Li X, Adair K R, Li J J, Wang C H, Yu C, Banis M N, Zhang L, Zhao S Q, Lu S G, Huang H, Li R Y, Huang Y N, Sun X L. $Li_{10}Ge(P_{1-x}Sb_x)_2S_{12}$ lithium-ion conductors with enhanced atmospheric stability[J]. Chem. Mat., 2020, 32(6): 2664−2672.

[42] Bonnick P, Niitani K, Nose M, Suto K, Arthur T S, Muldoon J. A high performance all solid state lithium sulfur battery with lithium thiophosphate solid electrolyte [J]. J. Mater. Chem., 2019, 7(42): 24173−24179.

[43] Tufail M K, Zhou L, Ahmad N, Chen R J, Faheem M, Yang L, Yang W. A novel air-stable $Li_7Sb_{0.05}P_{2.95}S_{10.5}I_{0.5}$ superionic conductor glass-ceramics electrolyte for all-

solid-state lithium-sulfur batteries[J]. J. Chem. Eng. Jpn., 2021, 407: 127149.

[44] Wu Z J, Xie Z K, Yoshida A, An X W, Wang Z D, Hao X G, Abudula A, Guan G Q. Novel SeS_2 doped Li_2S-P_2S_5 solid electrolyte with high ionic conductivity for all-solid-state lithium sulfur batteries[J]. J. Chem. Eng. Jpn., 2020, 380: 122419.

[45] Yu C, Hageman J, Ganapathy S, van Eijck L, Zhang L, Adair K R, Sun X L, Wagemaker M. Tailoring Li_6PS_5Br ionic conductivity and understanding of its role in cathode mixtures for high performance all-solid-state Li-S batteries[J]. J. Mater. Chem., 2019, 7(17): 10412−10421.

[46] Zhou L, Tufail M K, Ahmad N, Song T L, Chen R J, Yang W. Strong interfacial adhesion between the Li_2S cathode and a functional $Li_7P_{2.9}Ce_{0.2}S_{10.9}Cl_{0.3}$ solid-state electrolyte endowed long-term cycle stability to all-solid-state lithium-sulfur batteries[J]. ACS Appl. Mater. Interfaces, 2021, 13(24): 28270−28280.

[47] Wei C C, Yu C, Peng L F, Zhang Z Q, Xu R N, Wu Z K, Liao C, Zhang W, Zhang L, Cheng S J, Xie J. Tuning ionic conductivity to enable all-climate solid-state Li-S batteries with superior performances[J]. Mater. Adv., 2022, 3(2): 1047−1054.

[48] Zhu Y Z, He X F, Mo Y F. Origin of outstanding stability in the lithium solid electrolyte materials: insights from thermodynamic analyses based on first-principles calculations[J]. ACS Appl. Mater. Interfaces, 2015, 7(42): 23685−23693.

[49] Han F D, Zhu Y Z, He X F, Mo Y F, Wang C S. Electrochemical stability of $Li_{10}GeP_2S_{12}$ and $Li_7La_3Zr_2O_{12}$ solid electrolytes[J]. Adv. Energy Mater., 2016, 6(8): 1501590.

[50] Bai X T, Yu T W, Ren Z M, Gong S M, Yang R, Zhao C R. Key issues and emerging trends in sulfide all solid state lithium battery[J]. Energy Storage Mater., 2022, 51: 527−549.

[51] Zhang Z X, Zhang L, Yan X L, Wang H Q, Liu Y Y, Yu C, Cao X T, van Eijck L, Wen B. All-in-one improvement toward Li_6PS_5Br-based solid electrolytes triggered by compositional tune[J]. J. Power Sources, 2019, 410: 162−170.

[52] Wu F, Fitzhugh W, Ye L H, Ning J X, Li X. Advanced sulfide solid electrolyte by core-shell structural design[J]. Nat. Commun., 2018, 9: 4037.

[53] Nikodimos Y, Huang C J, Taklu B W, Su W N, Hwang B J. Chemical stability of sulfide solid-state electrolytes: stability toward humid air and compatibility with solvents and binders[J]. Energy Environ. Sci., 2022, 15(3): 991−1033.

[54] Jiang Z, Peng H L, Liu Y, Li Z X, Zhong Y, Wang X L, Xia X H, Gu C D, Tu J P. A versatile $Li_{6.5}In_{0.25}P_{0.75}S_5I$ sulfide electrolyte triggered by ultimate-energy mechanical alloying for all-solid-state lithium metal batteries[J]. Adv. Energy Mater., 2021, 11(36): 2101521.

[55] Tufail M K, Ahmad N, Zhou L, Faheem M, Yang L, Chen R J, Yang W. Insight on air-induced degradation mechanism of $Li_7P_3S_{11}$ to design a chemical-stable solid electrolyte with high Li_2S utilization in all-solid-state Li/S batteries[J]. Chem. Eng. J., 2021, 425: 130535.

[56] Yao X Y, Huang N, Han F D, Zhang Q, Wan H L, Mwizerwa J P, Wang C S, Xu X X. High-performance all-solid-state lithium-sulfur batteries enabled by amorphous sulfur-coated reduced graphene oxide cathodes[J]. Adv. Energy Mater., 2017, 7(17): 1602923.

[57] Wang S, Bai Q, Nolan A M, Liu Y S, Gong S, Sun Q, Mo Y F. Lithium chlorides and bromides as promising solid-state chemistries for fast ion conductors with good electrochemical stability[J]. Angew. Chem., Int. Ed., 2019, 58(24): 8039−8043.

[58] Emly A, Kioupakis E, Van der Ven A. Phase stability and transport mechanisms in antiperovskite Li_3OCl and Li_3OBr superionic conductors[J]. Chem. Mat., 2013, 25(23): 4663−4670.

[59] Shi X M, Zeng Z C, Sun M Z, Huang B L, Zhang H T, Luo W, Huang Y H, Du Y P, Yan C H. Fast Li-ion conductor of Li_3HoBr_6 for stable all-solid-state lithium-sulfur battery[J]. Nano Lett., 2021, 21(21): 9325−9331.

[60] Han F D, Yue J, Fan X L, Gao T, Luo C, Ma Z H, Suo L M, Wang C S. High-performance all-solid-state lithium-sulfur battery enabled by a mixed-conductive Li_2S nanocomposite[J]. Nano Lett., 2016, 16(7): 4521−4527.

[61] Zhang Q, Huang N, Huang Z, Cai L T, Wu J H, Yao X Y. CNTs@S composite as cathode for all-solid-state lithium-sulfur batteries with ultralong cycle life[J]. J. Energy Chem., 2020, 40: 151−155.

[62] Hou L P, Yuan H, Zhao C Z, Xu L, Zhu G L, Nan H X, Cheng X B, Liu Q B, He C X, Huang J Q, Zhang Q. Improved interfacial electronic contacts powering high sulfur utilization in all-solid-state lithium-sulfur batteries [J]. Energy Storage Mater., 2020, 25: 436−442.

[63] Li X N, Liang J W, Luo J, Wang C H, Li X, Sun Q, Li R Y, Zhang L, Yang R, Lu S G, Huang H, Sun X L. High-performance Li-SeS_x all-solid-state lithium batteries[J]. Adv. Mater., 2019, 31(17): 1808100.

[64] Tanibata N, Tsukasaki H, Deguchi M, Mori S, Hayashi A, Tatsumisago M. A novel discharge-charge mechanism of a S-P_2S_5 composite electrode without electrolytes in all-solid-state Li/S batteries[J]. J. Mater. Chem., 2017, 5(22): 11224−11228.

[65] Yao X Y, Liu D, Wang C S, Long P, Peng G, Hu Y S, Li H, Chen L Q, Xu X X. High-energy all-solid-state lithium batteries with ultralong cycle life[J]. Nano Lett., 2016, 16(11): 7148−7154.

[66] Sun X, Li Q, Cao D X, Wang Y, Anderson A, Zhu H L. High surface area N-doped carbon fibers with accessible reaction sites for all-solid-state lithium-sulfur batteries[J]. Small, 2022, 18(6): 2105678.

[67] Wang L, Yin X S, Li B, Zheng G W. Mixed ionically/electronically conductive double-phase interface enhanced solid-state charge transfer for a high-performance all-solid-state Li-S battery[J]. Nano Lett., 2022, 22(1): 433−440.

[68] Sakuda A, Sato Y, Hayashi A, Tatsumisago M. Sulfur-based composite electrode with interconnected mesoporous carbon for all-solid-state lithium-sulfur batteries [J]. Energy Technol., 2019, 7(12): 1900077.

[69] Dewald G F, Ohno S, Hering J GC, Janek J, Zeier W G. Analysis of charge carrier transport toward optimized cathode composites for all-solid-state Li-S batteries[J]. Batt. Supercaps, 2021, 4(1): 183−194.

[70] Liu Y Z, Meng X Y, Wang Z Y, Qiu J S. A Li_2S-based all-solid-state battery with high energy and superior safety[J]. Sci. Adv., 2022, 8(1): eabl8390.

[71] Gamo H, Maeda T, Hikima K, Deguchi M, Fujita Y, Kawasaki Y, Sakuda A, Muto H, Phuc N HH, Hayashi A. Synthesis of an AlI_3-doped Li_2S positive electrode with superior performance in all-solid-state batteries[J]. Mater. Adv., 2022, 3(5): 2488−2494.

[72] He Y M, Chen W J, Zhao Y M, Li Y F, Lv C Y, Li H X, Yang J G, Gao Z L, Luo J Y. Recent developments and progress of halogen elements in enhancing the performance of all-solid-state lithium metal batteries[J]. Energy Storage Mater., 2022, 49: 19−57.

[73] Wan H L, Zhang B, Liu S F, Zhang J X, Yao X Y, Wang C S. Understanding LiI-LiBr catalyst activity for solid state Li_2S/S reactions in an all-solid-state lithium battery[J]. Nano Lett., 2021, 21(19): 8488−8494.

[74] Jiang M, Liu G Z, Zhang Q, Zhou D, Yao X Y. Ultrasmall Li_2S-carbon nanotube nanocomposites for high-rate all-solid-state lithium-sulfur batteries[J]. ACS Appl. Mater. Interfaces, 2021, 13(16): 18666−18672.

[75] Jiang H Z, Han Y, Wang H, Zhu Y H, Guo Q P, Jiang H L, Zheng C M, Xie K. Facile synthesis of a mixed-conductive Li_2S composites for all-solid-state lithium-sulfur batteries [J]. Ionics, 2020, 26(9): 4257−4265.

[76] Wang D H, Wu Y Q, Zheng X F, Tang S J, Gong Z L, Yang Y. Li_2S @NC composite enable high active material loading and high Li_2S utilization for all-solid-state lithium sulfur batteries[J]. J. Power Sources, 2020, 479: 228792.

[77] Gao X, Zheng X L, Wang J Y, Zhang Z W, Xiao X, Wan J Y, Ye Y S, Chou L Y, Lee H K, Wang J Y, Vila R A, Yang Y F, Zhang P, Wang L W, Cui Y. Incorporating the nanoscale encapsulation concept from liquid electrolytes into solid-state lithium-sulfur batteries[J]. Nano Lett., 2020, 20(7): 5496−5503.

[78] Yan H F, Wang H C, Wang D H, Li X, Gong Z L, Yang Y. *In situ* generated Li_2S -C nanocomposite for high-capacity and long-life all-solid-state lithium sulfur batteries with ultrahigh areal mass loading[J]. Nano Lett., 2019, 19(5): 3280−3287.

[79] Jiang H Z, Han Y, Wang H, Zhu Y H, Guo Q P, Jiang H L, Sun W W, Zheng C M, Xie K. *In-situ* generated Li_2S-based composite cathodes with high mass and capacity loading for all-solid-state Li-S batteries[J]. J. Alloys Compd., 2021, 874: 159763.

[80] El-Shinawi H, Cussen E J, Corr S A. A facile synthetic approach to nanostructured Li_2S cathodes for rechargeable solid-state Li-S batteries[J]. Nanoscale, 2019, 11(41): 19297−19300.

[81] Li M Y, Pan H Y, Liu T, Xiong X L, Yu X Q, Hu Y S, Li H, Huang X J, Suo L M, Chen L Q. All-in-one ionic-electronic dual-carrier conducting framework thickening all-solid-state electrode[J]. ACS Energy Lett., 2022, 7(2): 766−772.

[82] Wan H L, Liu G Z, Li Y L, Weng W, Mwizerwa J P, Tian Z Q, Chen L, Yao X Y. Transitional metal catalytic pyrite cathode enables ultrastable four-electron-based all-solid-state lithium batteries[J]. ACS Nano, 2019, 13(8): 9551−9560.

[83] Xu S Q, Kwok C Y, Zhou L D, Zhang Z Z, Kochetkov I, Nazar L F. A high capacity all solid-state Li-sulfur battery enabled by conversion-intercalation hybrid cathode architecture[J]. Adv. Funct. Mater., 2021, 31(2): 2004239.

[84] Santhosha A L, Nazer N, Koerver R, Randau S, Richter F H, Weber D A, Kulisch J, Adermann T, Janek J, Adelhelm P. Macroscopic displacement reaction of copper sulfide in lithium solid-state batteries[J]. Adv. Energy Mater., 2020, 10(41): 2002394.

[85] Zhang Q, Ding Z G, Liu G Z, Wan H L, Mwizerwa J P, Wu J H, Yao X Y. Molybdenum trisulfide based anionic redox driven chemistry enabling high-performance all-solid-state lithium metal batteries[J]. Energy Storage Mater., 2019, 23: 168−180.

[86] Dewald G F, Liaqat Z, Lange M A, Tremel W, Zeier W G. Influence of iron sulfide nanoparticle sizes in solid-state batteries[J]. Angew. Chem., Int. Ed., 2021, 60(33): 17952−17956.

[87] Santhosha A L, Nayak P K, Pollok K, Langenhorst F, Adelhelm P. Exfoliated MoS_2 as electrode for all-solid-state rechargeable lithium-ion batteries[J]. J. Phys. Chem. C, 2019, 123(19): 12126−12134.

[88] Yamakawa N, Jiang M, Grey C P. Investigation of the conversion reaction mechanisms for binary copper(II) compounds by solid-state NMR spectroscopy and X-ray diffraction[J]. Chem. Mat., 2009, 21(14): 3162−3176.

[89] Hosseini S M, Varzi A, Ito S, Aihara Y, Passerini S. High loading CuS-based cathodes for all-solid-state lithium sulfur batteries with enhanced volumetric capacity[J]. Energy Storage Mater., 2020, 27: 61−68.

[90] Pan H, Zhang M H, Cheng Z, Jiang H Y, Yang J G, Wang P F, He P, Zhou H S. Carbon-free and binder-free Li-Al alloy anode enabling an all-solid-state Li-S battery with high energy and stability[J]. Sci. Adv., 2022, 8(15): eabn4372.

[91] Tan D HS, Chen Y T, Yang H D, Bao W, Sreenarayanan B, Doux J M, Li W K, Lu B Y, Ham S Y, Sayahpour B, Scharf J, Wu E A, Deysher G, Han H E, Hah H J, Jeong H, Lee J B, Chen Z, Meng Y S. Carbon-free high-loading silicon anodes enabled by sulfide solid electrolytes[J]. Science, 2021, 373(6562): 1494−1499.

[92] Chen Z R, Liang Z T, Zhong H Y, Su Y, Wang K J, Yang Y. Bulk/interfacial synergetic approaches enable the stable anode for high energy density all-solid-state lithium-sulfur batteries[J]. ACS Energy Lett., 2022, 7(8): 2761−2770.

[93] Shin M, Gewirth A A. Incorporating solvate and solid electrolytes for all-solid-state Li_2S batteries with high capacity and long cycle life[J]. Adv. Energy Mater., 2019, 9(26): 1900938.

[94] Sun X, Stavola A M, Cao D X, Bruck A M, Wang Y, Zhang Y L, Luan P C, Gallaway J W, Zhu H L. *Operando* EDXRD study of all-solid-state lithium batteries coupling thioantimonate superionic conductors with metal sulfide [J]. Adv. Energy Mater., 2021, 11(3): 2002861.

[95] Liu M, Wang C, Zhao C L, van der Maas E, Lin K, Arszelewska V A, Li B H, Ganapathy S, Wagemaker M. Quantification of the Li-ion diffusion over an interface coating in all-solid-state batteries via NMR measurements [J]. Nat. Commun., 2021, 12(1): 5943.

[96] Umeshbabu E, Zheng B Z, Zhu J P, Wang H C, Li Y X, Yang Y. Stable cycling lithium-sulfur solid batteries with enhanced $Li/Li_{10}GeP_2S_{12}$ solid electrolyte interface stability[J]. ACS Appl. Mater. Interfaces, 2019, 11(20): 18436−18447.

[97] Lou S F, Zhang F, Fu C K, Chen M, Ma Y L, Yin G P, Wang J J. Interface issues and challenges in all-solid-state batteries: lithium, sodium, and beyond[J]. Adv. Mater., 2021, 33(6): 2000721.

[98] Wan H L, Mwizerwa J P, Qi X G, Liu X, Xu X X, Li H, Hu Y S, Yao X Y. Core-shell $Fe_{1-x}S@Na_{2.9}PS_{3.95}Se_{0.05}$ nanorods for room temperature all-solid-state sodium batteries with high energy density[J]. ACS Nano, 2018, 12(3): 2809−2817.

[99] Shi J M, Liu G Z, Weng W, Cai L T, Zhang Q, Wu J H, Xu X X, Yao X Y. $Co_3S_4@Li_7P_3S_{11}$ hexagonal platelets as cathodes with superior interfacial contact for all-solid-state lithium batteries[J]. ACS Appl. Mater. Interfaces, 2020, 12(12): 14079−14086.

[100] Xu R C, Wang X L, Zhang S Z, Xia Y, Xia X H, Wu J B, Tu J P. Rational coating of $Li_7P_3S_{11}$ solid electrolyte on MoS_2 electrode for all-solid-state lithium ion batteries[J]. J. Power Sources, 2018, 374: 107−112.

[101] Sun N, Liu Q S, Cao Y, Lou S F, Ge M Y, Xiao X H, Lee W K, Gao Y Z, Yin G P, Wang J J, Sun X L. Anisotropically electrochemical-mechanical evolution in solid-state batteries and interfacial tailored strategy[J]. Angew. Chem., Int. Ed., 2019, 58(51): 18647−18653.

[102] Xu J, Liu L, Yao N, Wu F, Li H, Chen L. Liquid-involved synthesis and processing of sulfide-based solid electrolytes, electrodes, and all-solid-state batteries[J]. Mater. Today Nano, 2019, 8: 100048.

[103] Cao Y, Zuo P J, Lou S F, Sun Z, Li Q, Huo H, Ma Y L, Du C Y, Gao Y Z, Yin G P. A quasi-solid-state Li-S battery

with high energy density, superior stability and safety[J]. J. Mater. Chem., 2019, 7(11): 6533−6542.
[104] Lou S F, Liu Q W, Zhang F, Liu Q S, Yu Z J, Mu T S, Zhao Y, Borovilas J, Chen Y J, Ge M Y, Xiao X H, Lee W K, Yin G P, Yang Y, Sun X L, Wang J J. Insights into interfacial effect and local lithium-ion transport in polycrystalline cathodes of solid-state batteries[J]. Nat. Commun., 2020, 11(1): 5700.
[105] Zhu C B, Usiskin R E, Yu Y, Maier J. The nanoscale circuitry of battery electrodes[J]. Science, 2017, 358(6369): eaao2808.
[106] Hakari T, Fujita Y, Deguchi M, Kawasaki Y, Otoyama M, Yoneda Y, Sakuda A, Tatsumisago M, Hayashi A. Solid electrolyte with oxidation tolerance provides a high-capacity Li_2S-based positive electrode for all-solid-state Li/S batteries[J]. Adv. Funct. Mater., 2022, 32(5): 2106174.
[107] Kim S, Oguchi H, Toyama N, Sato T, Takagi S, Otomo T, Arunkumar D, Kuwata N, Kawamura J, Orimo S. A complex hydride lithium superionic conductor for high-energy-density all-solid-state lithium metal batteries[J]. Nat. Commun., 2019, 10: 1081.
[108] Kisu K, Kim S, Yoshida R, Oguchi H, Toyama N, Orimo S. Microstructural analyses of all-solid-state Li-S batteries using $LiBH_4$-based solid electrolyte for prolonged cycle performance[J]. J. Energy Chem., 2020, 50: 424−429.
[109] Ruan Y D, Lu Y, Huang X, Su J M, Sun C Z, Jin J, Wen Z Y. Acid induced conversion towards a robust and lithiophilic interface for Li-$Li_7La_3Zr_2O_{12}$ solid-state batteries[J]. J. Mater. Chem., 2019, 7(24): 14565−14574.
[110] Bosubahu D, Sivaraj J, Sampathkumar R, Ramesha K. Lagpili interface modification through a wetted polypropylene interlayer for solid state Li-ion and Li-S batteries[J]. ACS Appl. Energy Mater., 2019, 2(6): 4118−4125.
[111] Judez X, Eshetu G G, Gracia I, Lopez-Aranguren P, Gonzalez-Marcos J A, Armand M, Rodriguez-Martinez L M, Zhang H, Li C M. Understanding the role of nano-aluminum oxide in all-solid-state lithium-sulfur batteries[J]. Chemelectrochem, 2019, 6(2): 326−330.
[112] Yin X S, Wang L, Kim Y, Ding N, Kong J H, Safanama D, Zheng Y, Xu J W, Repaka D VM, Hippalgaonkar K, Lee S W, Adams S, Zheng G W. Thermal conductive 2D boron nitride for high-performance all-solid-state lithium-sulfur batteries[J]. Adv. Sci., 2020, 7(19): 2001303.
[113] Fan Z J, Ding B, Zhang T F, Lin Q Y, Malgras V, Wang J, Dou H, Zhang X G, Yamauchi Y. Solid/solid interfacial architecturing of solid polymer electrolyte-based all-solid-state lithium-sulfur batteries by atomic layer deposition[J]. Small, 2019, 15(46): 1903952.
[114] Li J, Huo F, Chen T H, Yan H W, Yang Y X, Zhang S J, Chen S M. *In-situ* construction of stable cathode/Li interfaces simultaneously via different electron density AZO compounds for solid-state lithium metal batteries[J]. Energy Storage Mater., 2021, 40: 394−401.

固态锂硫电池研究进展

罗　宇[a,#]，马如琴[a,#]，龚正良[b,*]，杨　勇[a,b,*]
[a]厦门大学固体表面物理化学国家重点实验室，化学化工学院，福建 厦门 361005
[b]厦门大学能源学院，福建 厦门 361005

摘要

固态锂硫电池具有高能量密度和高安全性的潜在优势，被认为是最有前景的下一代储能体系之一。虽然固态电解质的应用有效地抑制了传统锂硫电池存在的“穿梭效应”和自放电现象，固态锂硫电池仍面临着多相离子/电子输运、电极/电解质界面稳定性、化学-机械稳定性、电极结构稳定性和锂枝晶生长等关键问题亟待解决。针对以上问题，本综述对近年来固态电解质、硫基复合正极、锂金属及锂合金负极以及电极/电解质界面的研究进行了详细的论述。作为固态锂硫电池的重要组成部分，固态电解质近年来受到了研究者们的广泛关注。本文首先对在锂硫电池中得到广泛应用的聚合物基、氧化物基、硫化物基固态电解质的种类和性质进行了概述，并对其在固态锂硫电池中的最新应用进行了系统的总结。在此基础上，对以单质硫、硫化锂、金属硫化物为活性物质的复合硫正极、锂金属及锂合金负极的反应机理以及面临的挑战进行了归纳和比较，对其解决策略进行了总结和分析。此外，对制约固态锂硫电池性能的电极/电解质界面离子/电子输运以及界面相容性问题及其改性策略进行了系统的阐述。最后，对固态锂硫电池的未来发展进行了展望。

关键词：锂硫电池；固态电解质；界面相容性；三相界面；电化学-机械应力